APPLICATIONS OF AN ELECTRONIC TRANSFORMER IN A POWER DISTRIBUTION SYSTEM

A Dissertation

by

SOMNIDA RATANAPANACHOTE

Submitted to the Office of Graduate Studies of
Texas A&M University
in partial fulfillment of the requirements for the degree of

DOCTOR OF PHILOSOPHY

August 2004

Major Subject: Electrical Engineering

APPLICATIONS OF AN ELECTRONIC TRANSFORMER

IN A POWER DISTRIBUTION SYSTEM

A Dissertation

by

SOMNIDA RATANAPANACHOTE

Submitted to Texas A&M University
in partial fulfillment of the requirements
for the degree of

DOCTOR OF PHILOSOPHY

Approved as to style and content by:

Prasad Enjeti (Chair of Committee)	
Chanan Singh (Member)	Donald Smith (Member)
Henry Taylor (Member)	Chanan Singh (Head of Department)

August 2004

Major Subject: Electrical Engineering

ABSTRACT

Applications of an Electronic Transformer in a Power Distribution System.

(August 2004)

Somnida Ratanapanachote,

B.Eng., Mahidol University, Bangkok, Thailand;

M.Eng., Texas A&M University

Chair of Advisory Committee: Dr. Prasad N. Enjeti

In electrical power distribution and power electronic applications, a transformer is an indispensable component which performs many functions. At its operating frequency (60/50 Hz), it is one of the most bulky and expensive components. The concept of the electronic transformer introduced previously has shown considerable reduction in size, weight, and volume by operating at a higher frequency.

In this dissertation, the concept of the electronic transformer is further extended to the auto-connected phase-shifting type to reduce harmonics generated by nonlinear loads. It is shown that with the addition of primary side and secondary side AC/AC converters achieves phase-shifting. With the addition of converters, magnetic components are operated at a higher frequency to yield a smaller size and weight. Two types of auto-connected electronic transformer configurations are explored. In the first configuration, the secondary converter is eliminated and the output is suitable for rectifier type loads such as adjustable speed drives. In the second configuration, the

secondary converter is added to obtain a sinusoidal phase-shifted AC output voltage. This approach is applicable in general applications. With the proposed approaches, the 5^{th} and 7^{th} harmonic in utility line currents, generated by two sets of nonlinear loads, are subtracted within the electronic transformer, thereby reducing the total harmonic distortion (THD) of the line current. The analysis and simulation results are presented.

In the second part of the dissertation, the electronic transformer concept is applied to a telecommunication power supply (-48 VDC) system. The proposed approach consists of a matrix converter to convert the low frequency three-phase input AC utility to a high frequency AC output without a DC-link. The output of the matrix converter is then processed via a high frequency isolation transformer to produce -48 VDC. Digital control of the system ensures that the output voltage is regulated and the input currents are of high quality, devoid of low frequency harmonics and at near unity input power factor under varying load conditions. Due to the absence of DC-link electrolytic capacitors, the power density of the proposed rectifier is shown to be higher. Analysis, design example and experimental results are presented from a three-phase 208 V, 1.5 kW laboratory prototype converter.

To my beloved parents

Sompoch and Panida

ACKNOWLEDGMENTS

Above all, I am so grateful for every blessing, strength, and guidance that comes from God.

I would like to express my gratitude to Dr. Prasad Enjeti, who has been a great mentor and never gives up on me. I am so thankful for his support and encouragement throughout my health problem. His guidelines and wisdom are so much appreciated.

I also would like to thank my committee members, Dr. Chanan Singh and Dr. Henry Taylor, for their valuable comments and time, and Dr. Donald Smith, I thank you for the long casual conversations that give me various views of life.

To Hanju Cha and Chutt, who are always helpful and generous, I thank you for all of the advice and assistance.

Special thanks to my wonderful parents and family who always believe in me. Your unconditional love helps me overcome any difficulty. I also thank Ohm, my best friend, who is always by my side through ups and downs, and makes me feel so special. To Bob, Myrt, Kelly and Sara Davidson, thank you all so much for helping me settle down when I first arrived and always opening your home with a warm welcome for me. I would like to also give thanks to Dr. Ann Reed, Dr. Ron Lutz, Ms. Linda Kapusniak, and Ms. Karen Beathard, who kindly took good care of me through my health recovery so I could focus on my studies again.

To all of my friends at Texas A&M University, I thank you all for being great companions. And to all my friends from home, thank you for encouraging me.

TABLE OF CONTENTS

Page

ABSTRACT iii

DEDICATION iv

ACKNOWLEDGMENTS vi

TABLE OF CONTENTS vii

LIST OF FIGURES x

LIST OF TABLES xiii

CHAPTER

I INTRODUCTION 1

1.1 Introduction 1
1.2 Previous work 2
1.2.1 Solid state transformer 3
1.2.2 Phase-shifting transformer 4
1.2.3 Telecommunication power supply 7
1.3 Research objectives 8
1.4 Scope of the dissertation 10

II ELECTRONIC TRANSFORMER 11

2.1 Introduction 11
2.2 Development of intelligent universal transformer 12
2.3 High frequency transformer 13
2.3.1 Core loss 14
2.3.2 Copper loss and skin effect 15
2.4 Electronic transformer system 17
2.4.1 Topology of electronic transformer 18
2.4.2 Analysis of electronic transformer 21
A. Single phase electronic tranformer system 21
B. Three-phase electronic tranformer system 25
2.4.3 4-step switching strategy 27
A. Voltage reference mode 28
B. Current reference mode 30

CHAPTER Page

2.5 Electronic transformer applications in power distribution system 32
2.6 Conclusion....35

III AUTO-CONNECTED ELECTRONIC PHASE-SHIFTING TRANSFORMER IN ELECTRICAL POWER DISTRIBUTION SYSTEM....36

3.1 Introduction....36
3.2 Proposed topology....39
3.3 Analysis of the proposed topology....42
3.3.1 Voltage analysis....42
3.3.2 Current analysis....44
A. Balanced nonlinear load....44
B. Unbalanced nonlinear load....45
3.4 Design example....49
3.5 Simulation results....49
3.6 Conclusion....58

IV ELECTRONIC TRANSFORMER APPLICATION IN TELECOMMUNICATION POWER SUPPLY....59

4.1 Introduction....59
4.2 Proposed switch mode power supply....60
4.3 Matrix converter PWM modulation....62
4.3.1 Rectifier mode of operation....64
4.3.2 Inverter mode of operation....66
4.3.3 Proposed switching modulation....68
4.4 Analysis of the proposed power conversion stage....70
4.4.1 Voltage analysis....70
4.4.2 Line current and harmonic analysis....72
4.5 Design example....74
4.5.1 Input filter design....76
4.6 Simulation results....77
4.7 Experimental results....80
4.8 Conclusion....83

V CONCLUSION....84

Page

REFERENCES 87

APPENDIX 91

VITA 92

LIST OF FIGURES

FIGURE Page

1.1 Schematic of solid state transformer 3

1.2 Block diagram of electronic transformer..... 4

1.3 Phase-shifting transformer in electrical power distribution system..... 5

1.4 Diagram of 30º phase-shifting transformer 6

1.5 12-pulse auto-connected transformer system 7

1.6 Typical telecommunication power supply..... 8

2.1 EPRI intelligent universal transformer (IUT layout) 12

2.2 Topologies of single phase electronic transformer system.....18

2.3 Topologies of three-phase electronic transformer system.....20

2.4 Switching function for single phase electronic transformer system 22

2.5 Single phase electronic transformer system voltages.....23

2.6 Single phase electronic transformer system currents 24

2.7 Three-phase electronic transformer system voltages 26

2.8 Example of gate signals by 4-step switching voltage reference mode.....28

2.9 Example of gate signals by 4-step switching current reference mode 30

2.10 Block diagram of gating signal selection through FPGA.....32

2.11 Single phase distribution transformer 34

3.1 Circuit diagram of the polyphase autotransformer 37

3.2 Proposed auto-connected electronic transformer for cancelling 5^{th} and 7^{th} harmonics generated in rectifier loads 39

3.3 Vector diagram of phase-shifting autotransformer 40

FIGURE Page

3.4 The alternative auto-connected electronics phase-shifting transformer topology 41

3.5 Utility line current THD in per-unit at unbalanced loads 48

3.6 Input line-to-neutral voltages, V_{an}, V_{bn}, and V_{cn} at 60 Hz 50

3.7 High frequency voltages on transformer primary side 51

3.8 Spectrums of high frequency voltages on transformer primary side 51

3.9 Input voltages of the rectifier type nonlinear loads 52

3.10 Input currents of the rectifier type nonlinear loads 53

3.11 Spectrums of input currents of the rectifier type nonlinear loads 53

3.12 Input line currents, I_a, I_b, and I_c of topology in Fig.3.2 54

3.13 Spectrums of input line currents (5^{th} and 7^{th} harmonics are cancelled) of topology in Fig.3.2 54

3.14 Input voltages of the nonlinear loads without high frequency components 55

3.15 Input currents of the nonlinear loads 55

3.16 Spectrums of input currents of nonlinear loads 56

3.17 Input line currents, I_a, I_b, and I_c of topology in Fig.3.4 56

3.18 Spectrums of input line currents (5^{th} and 7^{th} harmonics are cancelled) of topology in Fig.3.4 57

3.19 The graphical results of THD percentage at different unbalanced loads 58

4.1 Conventional telecommunication switch mode power supply 60

4.2 Proposed digitally controlled switch mode power supply based on matrix converter 61

FIGURE Page

4.3 EUPEC 18-IGBT switch module for matrix converter implementation.....62

4.4 A figure of three-phase to single phase matrix converter.....63

4.5 Illustration of matrix converter operation.....63

4.6 Rectifier space vector hexagon 65

4.7 Inverter mode switching function 67

4.8 Block diagram of the proposed matrix converter modulation 69

4.9 Matrix converter switch gating signals generating through logic gates.....70

4.10 %THD of input line currents at different input line voltages 74

4.11 The three-phase input voltages V_{ab}, V_{bc}, and V_{ca} : 208 V (rms) 60 Hz 77

4.12 High frequency output voltage V_{pri} of the matrix converter 78

4.13 Output DC voltage (48 V) 78

4.14 Input line to neutral input voltage V_{an} and input current I_a 79

4.15 THD percentage at different loads 79

4.16 Proposed Matrix converter prototype.....81

4.17 Input voltage V_{ab}, matrix converter output voltage V_{pri}, and transformer secondary voltage V_{sec} 81

4.18 Transformer primary V_{pri} and secondary voltages V_{sec} 82

4.19 Output DC voltage V_{dc} and load current I_{dc} 82

4.20 Input line to neutral voltage V_{an} and the input line current I_a at 1.5 kW of output power.....83

LIST OF TABLES

TABLE Page

2.1 Number of semiconductor switches used in electronic transformer system 21

2.2 Voltage reference 4-step switching sequence 29

2.3 Current reference 4-step switching sequence 31

3.1 VA rating of the system 49

4.1 %THD of input line currents at different input line voltages 73

4.2 Design specifications of the proposed approach 75

CHAPTER I

INTRODUCTION

1.1 Introduction

A transformer is a static device consisting of a winding, or two or more coupled windings, with different number of turns on a magnetic core, for inducing mutual coupling between circuits. The alternating current magnetic field created in one winding induces a current in the other in proportional to the number of turns. Transformers are exclusively used in electrical power systems to transfer power by electromagnetic induction between circuits at the same frequency with very little power loss, voltage drop or waveform distortion.

Transformers are important equipment in power distribution system as well as in power electronic system. They can step down high voltages in transmission at substations or step up currents to the needed level of end-users. Additionally, many functions, for instance, isolation, noise decoupling or phase-shifting can be achieved through transformers.

A low frequency (60/50 Hz) transformer is one the most bulky and expensive components in electrical power system. There have been inclusive studies to reduce size and weight of the transformer.

This dissertation follows the style of *IEEE Transactions on Power Electronics.*

The size of a transformer is a function of the saturation flux density or core material, current density of conductor, and operating frequency of excitation. Therefore, employing high current density wire materials, such as high temperature super-conductor or employing advanced core materials, such as a finer grade of steel or an amorphous, which has higher saturation flux density, can reduce the size and weight of a transformer.

The saturation flux density is inversely proportional to frequency. Therefore, the size reduction can be achieved by increasing frequency through a static converter. Development of power electronic converters and switching devices advance as high frequency link system is researched. The study shows concerns on high EMI and losses.

Electronic transformer, with concept of a high frequency AC link, is introduced in reference [1]. More studies on electronic transformer have been done and published in the past many years. In this dissertation, the concept of electronic transformer is further explored. Proposed electronic transformer applications are also presented.

1.2 Previous work

As discussed in section 1.1, operating magnetic core at high frequency is an approach to reduce the size and weight of transformers. The electronic transformer concept, which magnetic core operates at high frequency, has been applied to phase-shifting transformer and telecommunication power supply applications.

1.2.1 Solid state transformer

Solid state transformer is introduced to reduce the size of transformer through high operating frequency [2]. An example of solid state transformer system is shown in Fig. 1.1.

At input stage, low frequency input is rectified to DC voltage, and the boost converter increases the DC voltage level for power factor correction. During the isolation stage, boosted DC voltage is converted to high frequency AC voltage by an inverter. The high frequency operation allows the reduction in size and weight of the isolation transformer. The high frequency AC voltage is rectified and converted to the desired AC voltage by an inverter in the output stage.

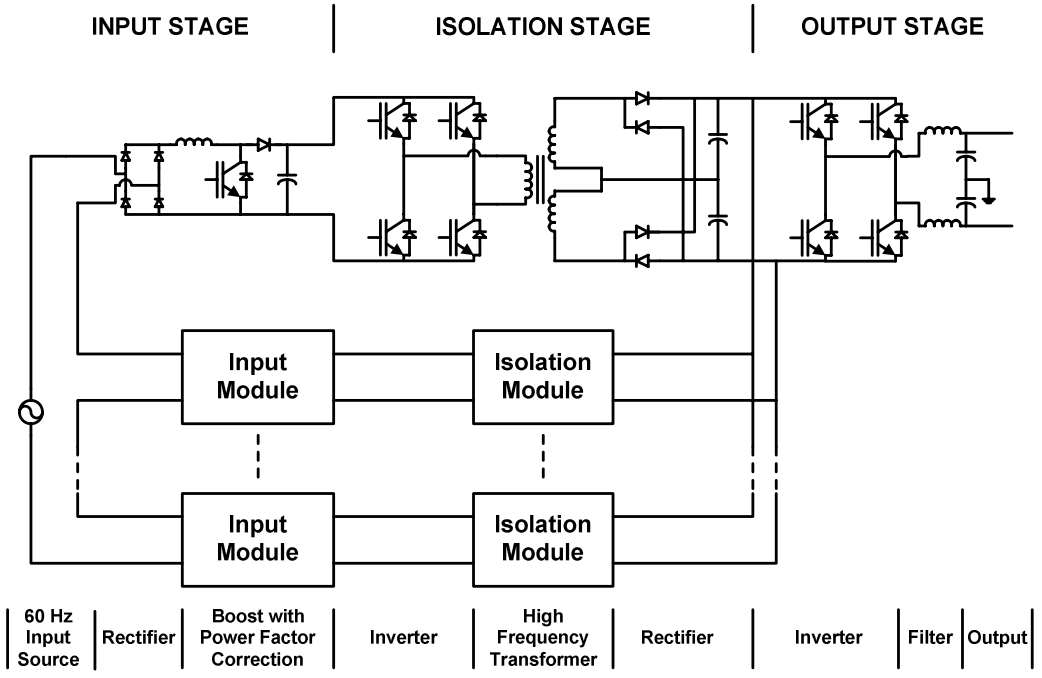

Fig. 1.1. Schematic of solid state transformer.

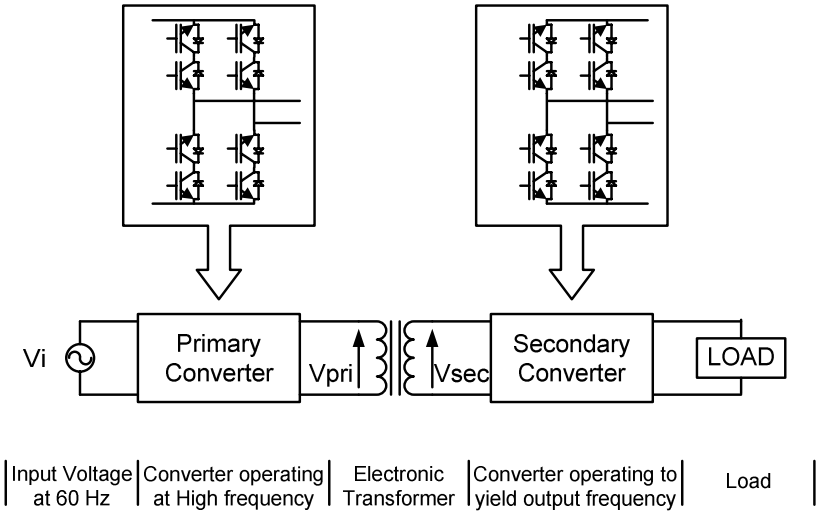

Fig. 1.2. Block diagram of electronic transformer.

Recent progress in high power switching devices, an electronic transformer is introduced as shown in Fig. 1.2. Multi-stage power conversion can be reduced by applying an AC/AC converter on each primary or secondary side of the transformer. Desired frequency of AC voltage can be achieved through AC/AC converter.

1.2.2 Phase-shifting transformer

A phase-shifting transformer is a special type of three-phase transformer that shifts the phase angle between the incoming and outgoing lines without changing the voltage ratio [3].

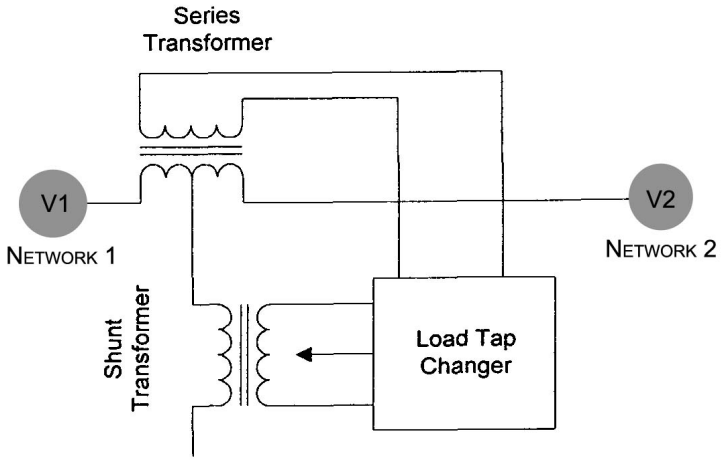

Fig. 1.3. Phase-shifting transformer in electrical power distribution system [4].

In electrical distribution system, the phase-shifting transformer as shown in Fig. 1.3, is introduced to control transmission voltage and phase angle of the system. Power system theory shows that, when power flows between two networks, there is a voltage drop and a phase angle shift between the sending end and the receiving end voltages. If the systems are connected together in two or more parallel paths so that a loop exists, any difference in the impedances will cause unbalanced line loading. Inserting the phase-shifting transformer into the transmission lines enables power flow control through a phase-shift tap changer and voltage tap changer [5].

Multi-pulse method involves multi-pulse converters connected to cancel several lower harmonic components in the input line current. Phase-shifting transformer is an essential component to provide the harmonic cancellation. Certain harmonics are eliminated from power source depending on number of converters [6]. Through windings on primary and secondary sides of the transformer, phase-shifting

angle is created. Fig. 1.4 shows a diagram of delta/wye/delta transformer, which each secondary winding feeds separate converter load. One load is fed through a delta/wye transformer, while another load is fed through delta/delta transformer. The 30º phase-shifting angle is produced. If the converter loads are equal, certain harmonics are eliminated from the utility.

Later, auto-connected transformer concept is introduced to reduce the VA rating of the transformer used in multi-pulse converter system [7], [8]. A 12-pulse auto-connected transformer system is shown in Fig. 1.5.

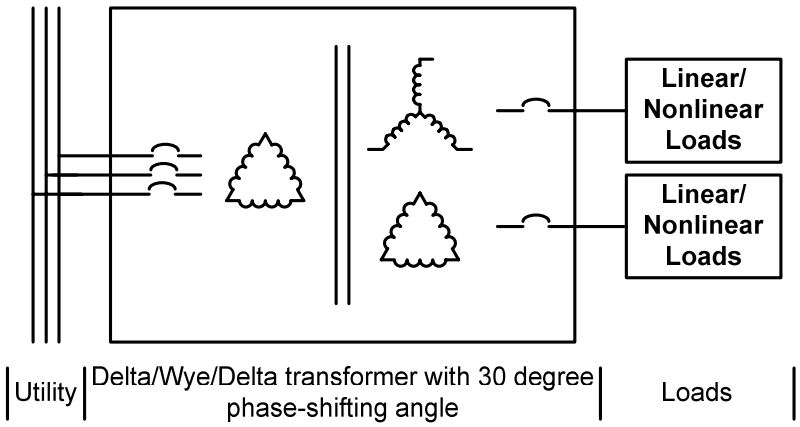

Fig. 1.4. Diagram of 30º phase-shifting transformer.

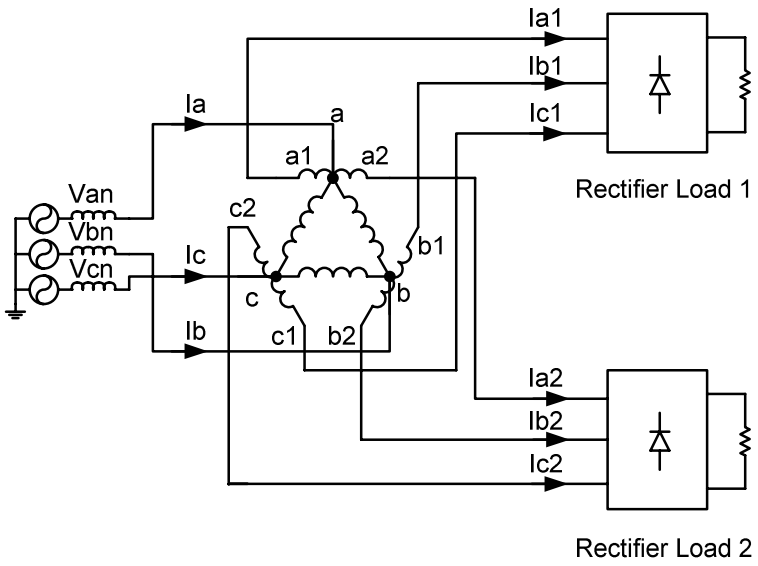

Fig. 1.5. 12-pulse auto-connected transformer system.

The transformer provides necessary phase-shift between 2 separate converter loads. The phase-shifting angle is chosen such that certain harmonics are cancelled in input line current. The mentioned phase-shifting transformer system is suitable for low frequency (60/50 Hz) transformer.

1.2.3 Telecommunication power supply

High power telecommunication power supply systems consist of a three-phase switched mode rectifier followed by a DC/DC converter to supply load at -48 VDC as shown in Fig. 1.6.

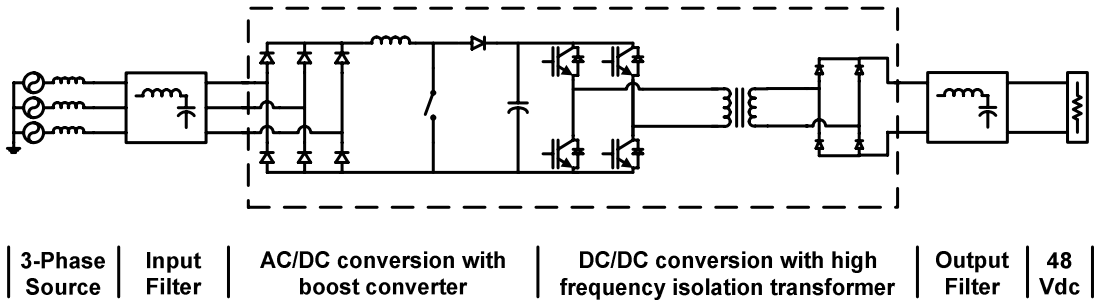

Fig. 1.6. Typical telecommunication power supply.

Modern telecommunication power systems require several rectifiers in parallel to obtain higher DC power with -48 VDC [9]. Such a rectifier normally employs diodes or silicon-controlled rectifiers to interface with the electric utility due to economic reasons. The rectifier type utility interface causes significant harmonic currents resulting in poor input power factor and high total harmonic distortion (THD), which contributes to an inefficient use of electric energy. The mentioned rectifier is referred to as nonlinear loads. The proliferation of rectifier loads deteriorates the quality of voltage and current waveforms. Further, harmonic currents can lead to equipment over heating, malfunction of solid-state equipment, and interference with communication systems.

1.3 Research objectives

The main objective of the research is to reduce the size and weight of the magnetic components in power distribution and conversion systems. New technique of high frequency conversion system is developed and applied to reach the purpose.

The concept of electronic transformers is explored to suit in power distribution and conversion systems. It is noted that the proposed electronic transformer and the conventional transformer performances are identical. Possible topologies employing static converters connected on the primary and/or secondary sides are explored to realize high frequency operation of the transformer magnetic core. Reducing number of converter switches are considered as switch configurations including matrix converter concept are discussed. To assist with commutation process, a 4-step switching is developed for snubber-less operation. Reduce size, losses, and higher efficiency are some of the advantages of the approach.

The concept of the electronic transformer is applied to an auto-connected electronic phase-shifting transformer approach. The proposed system achieves cancellation of 5^{th} and 7^{th} harmonics in utility line currents, which are generated by nonlinear load. The system is considerable in size and weight reduction due to the high frequency operation of transformer magnetic core. Analysis and simulation results of the proposed approach are presented.

Finally, the electronic transformer is proposed to telecommunication power supply system. A matrix converter is applied to realize high frequency operation of the transformer magnetic core. The direct AC to AC conversion capability of the matrix converter can replace multiple power conversion stages in conventional power supply. Matrix converter modulation is established to regulate required output voltage and improve power quality of utility line currents. Digital signal processor (DSP) is

chosen for feedback control. Design example along with the simulation and experimental results are presented.

1.4 Scope of the dissertation

The content of this dissertation is organized in the following manner. In CHAPTER I, the background information about power distribution transformer and their trend are discussed. Previous works of transformer size reduction and applications of transformer in power electronic systems are explained.

In CHAPTER II, design of high frequency transformer is discussed. The effect of high frequency operation on the transformer core and winding are discussed and possible solutions are presented.

In CHAPTER III, an auto-connected electronic phase-shifting transformer concept is explored. Possible topologies are presented along with mathematical analysis. Design example and simulation results are included.

In CHAPTER IV, an electronic transformer application in telecommunication power supply is presented. A new topology applying matrix converter is discussed along with system analysis and simulation results. Design example and experimental results of prototype system are included.

In CHAPTER V, conclusions are given.

CHAPTER II

ELECTRONIC TRANSFORMER

2.1 Introduction

Transformers are widely used in electrical power distribution and power conversion systems to perform many functions, such as isolation, voltage transformation, noise decoupling, etc. Transformers are one of the most bulky and expensive parts in a power distribution and power conversion systems. The size of transformer is a function of saturation flux density of the core material and maximum allowable core and winding temperature rise. Saturation flux density is inversely proportional to frequency and increasing the frequency allows higher utilization of the steel magnetic core and reduction in transformer size. The subject of a high frequency link has been studied extensively in power electronic systems. Electronic transformer with concept of a high frequency AC link is introduced in [1].

In this chapter, an ongoing project on electronic transformer is introduced. The advantages of the proposal are stated. The concept of the high frequency AC link is further explored. The focus of this chapter is to realize an electronic transformer as a power delivery component in electrical distribution systems. The primary purpose is to reduce the size and weight and volume and to improve efficiency.

2.2 Development of Intelligent Universal Transformer

Electrical Power Research Institute (EPRI) has been researching on Intelligent Universal Transformer (IUT) [10]. It is proposed to replace conventional distribution transformer with the state-of-the-art power electronic system. An intelligent and controllable system can provide multiple transformer functions, such as voltage transformation, voltage regulation, non-standard customer voltages (DC or 400 Hz AC), voltage sag correction, power factor control, and distribution system status monitoring to facilitate automation. The IUT will be a foundation of Advanced Distribution Automation (ADA) that will transform distribution systems into multi-functional power exchange systems.

The IUT assembly layout is shown as block diagram in Fig. 2.1. The layout is based on solid state transformer previously discussed in CHAPTER I. It requires 2 power conversion stages: rectifying stage and inverting stage.

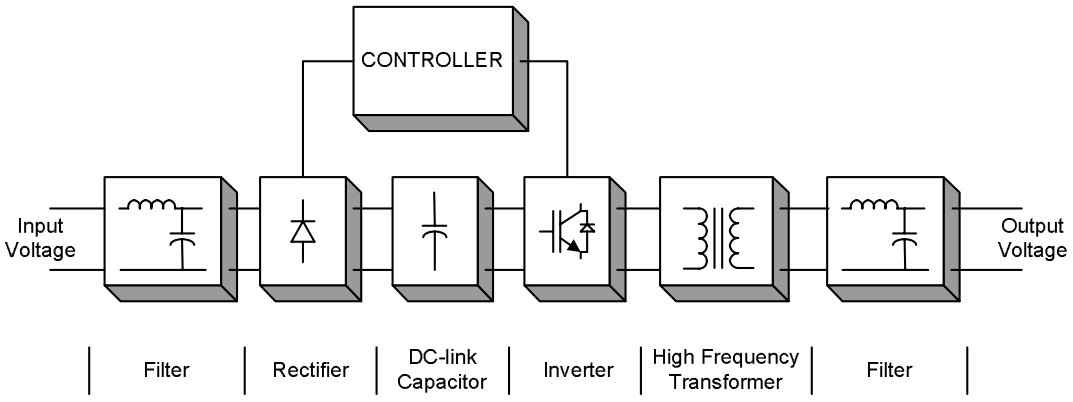

Fig. 2.1. EPRI intelligent universal transformer (IUT) layout.

The advantages of the IUT over conventional distribution transformer are:

- Improved power quality.
- DC and alternative frequency AC service options.
- Integration with system monitoring, advanced distribution automation and open communication architecture.
- Reduced weight and size.
- Elimination of hazardous liquid dielectrics.
- Reduced spare inventories.

To make the IUT possible, an advanced high-voltage power electronic circuit topology and a family of high-voltage, low-current power semiconductors (switching devices and diodes) have to be developed. Additionally, the IUT must have a standardized information model, as embedded software, which makes the IUT compatible with standardized open utility communication architecture.

Some drawbacks of the approach can be stated as followed:

- Multiple power conversion stages can lower the transformer efficiency.
- DC-link capacitors are required.
- The transformer lifetime is shorter due to storage devices.

2.3 High frequency transformer

As mentioned in previous chapter, a transformer can be designed in small size by operating transformer core at high frequency. The high frequency transformer shows significantly different characteristics from the low frequency transformer. Core

selection requires relationship between available output power and transformer parameters, such as core area product, peak flux density, operating frequency, and coil current density. Operating magnetic core at high frequency causes increase in core and copper losses.

2.3.1 Core loss

Eddy current loss (P_e) and hysteresis loss (P_h) are defined as core losses. Eddy current loss is power dissipated from eddy current generated in the conductive core. It is similar to the loss occurred in a short-circuited winding around the core. All magnetic cores exhibit some degree of hysteresis in their B-H characteristic. A typical B-H loop shows the rising and falling of magnetization curve, varying from one magnetic material to another. Hysteresis loss is energy dissipated in the magnetic material, which increases temperature of the material. The losses increase proportionally to operating frequency according to the following expressions, respectively.

$$P_e = K \frac{d^2 f_{sw}{}^2 B^2}{\rho} \tag{2.1}$$

$$P_h = K f_{sw}{}^a B^n \tag{2.2}$$

where K, a, and n are constants of core material.

f_{sw} is switching frequency.

B is flux density.

ρ is core resistivity.

d is lamination thickness.

To control eddy current loss at low to medium operating frequency, flux and induced voltage are reduced by subdividing magnetic core into lamination. At higher operating frequency, the thickness of laminated magnetic core should be small that causes difficulty. Ferrite is selected materials in high operating frequency since it suppresses eddy current by its high electrical resistivity and low saturation flux density. Generally, magnetic core manufacturing provides information of relationship between operating frequency and other characteristics for optimum material selection.

2.3.2 Copper loss and skin effect

The conductor windings in a transformer are made from copper due to its high conductivity. High conductivity contributes to minimizing the amount of copper needed for the windings and thus to the volume and weight of the winding. At the current density used in transformer, electrical loss is a significant source of heat even though the conductivity of copper is large. The heat generated raises the temperature of both the windings and magnetic core. The amount of dissipation allowable in the windings will be limited by maximum temperature considerations [11].

The winding loss due to DC resistance is not affected by the operating frequency as expressed in (2.3), but there are other effects that can generate winding losses.

$$P_w = K\rho J^2 \tag{2.3}$$

where K is copper fill factor.

ρ is copper resistivity.

J is current density in the conductor.

Skin effect is caused by eddy currents induced in a copper conductor by the magnetic fields of current carried by the conductor itself. The direction of these eddy currents is opposite to the main current flow on the inner of the conductor that result in magnetic field and also tend to shield the inner of the conductor from the main current to flow. Consequently, the current density is largest at the surface of the conductor, and the current flow only in a thin skin on the outer side of the conductor. The skin depth (δ), defined as the distance below the surface where the current density decay exponentially, is inversely proportional to square root of operating frequency according to (2.4).

$$\delta = \sqrt{\frac{2}{\omega\mu\sigma}} \tag{2.4}$$

where ω is angular operating frequency.

μ is magnetic permeability.

σ is the conductivity of the magnetic material.

As the operating frequency increases, the applied current mostly flows on the thin layer at the surface of the conductor. Therefore, the AC resistance causes winding loss. The solution of the problem is to decrease diameter of conductor used for winding. A special conductor arrangement for high frequency operation is developed such as Litz wire.

Litz wire is a connection of several electrically insulated small diameter wires in parallel. The wires must be twisted or woven into ropelike assembly in which each individual wire periodically moves from the inner to the outer of the conductor assembly. All the wires are connected in parallel only at the terminals of the transformer, which are located outside the winding.

2.4 Electronic transformer system

As mentioned in CHAPTER I, electronic transformer with concept of a high frequency AC link is introduced in [1]. The electronic transformer system consists of static AC/AC power converters applying to primary and/or secondary windings of the transformer as shown in Fig 1.2. Each converter contains bi-directional switches, which provide bi-directional energy flow. The low frequency (60/50 Hz) input voltage is converted to desired high operating frequency voltage through the primary converter, then the secondary converter restores the original low frequency input voltage. The secondary converter is optional. It is needed when the transformer supplies linear load type, and the operation requires both primary and secondary side

static converters to operate synchronously. The subject of high frequency AC link has been studied widely in power electronic systems.

The electronic transformer has advantages as followed [1].

- Identical input and output characteristic as a conventional transformer.
- Efficiency compatible with a conventional transformer.
- Snubber-less operation through 4-step switching strategy.
- No additional harmonics generated due to switching.
- Significantly smaller size and weight than a conventional transformer.

2.4.1 Topology of electronic transformer

Topologies of single phase electronic transformer system are shown in Fig. 2.2. Single phase AC/AC converters are applied to primary and secondary windings of a transformer.

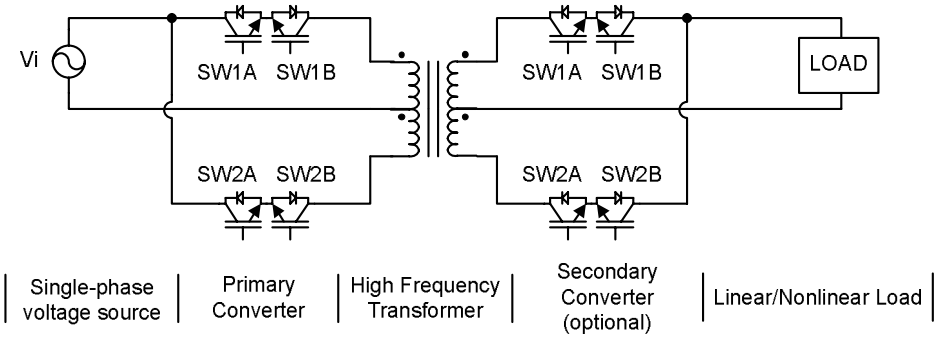

(a) Half-bridge single phase electronic transformer system.

Fig. 2.2. Topologies of single phase electronic transformer system.

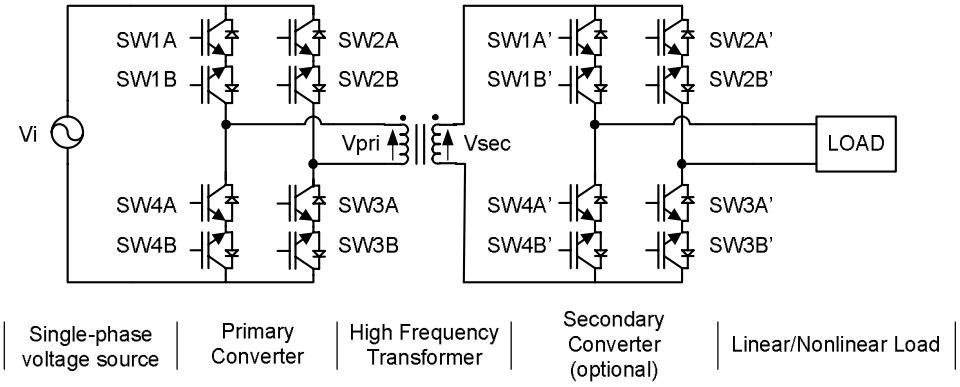

(b) Full-bridge single phase electronic transformer system.

Fig. 2.2. Continued.

Fig. 2.2 (a) shows the topology of single phase electronic transformer system, which includes AC/AC converters with bi-directional switches connecting in half-bridge arrangement. Fig. 2.2 (b) shows the topology of single phase electronic transformer system, which includes AC/AC converters with bi-directional switches connecting in full-bridge arrangement. The topology in Fig. 2.2 (a) requires the least number of bi-directional switches, but larger size of transformer than the topology shown in Fig. 2.2 (b). Topology of a three-phase electronic transformer system is shown in Fig. 2.3. The system consists of a high frequency transformer with open delta connection. Single phase AC/AC converters are selected to generate high frequency voltages on transformer primary windings. On the transformer secondary side, single phase AC/AC converters restore the voltages with input frequency. With this topology, the three-phase electronic transformer system can produce sinusoidal output voltages with no additional filter is required.

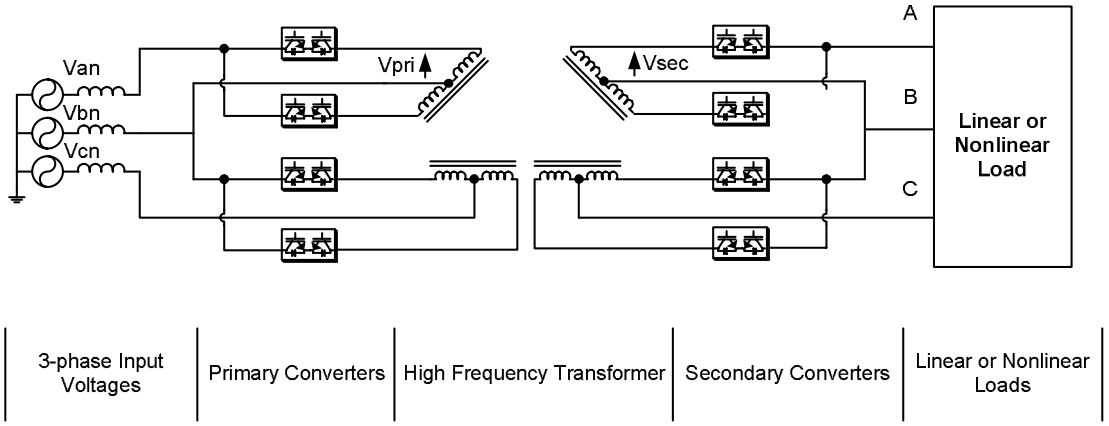

(a) Half-bridge open delta three-phase electronic transformer system.

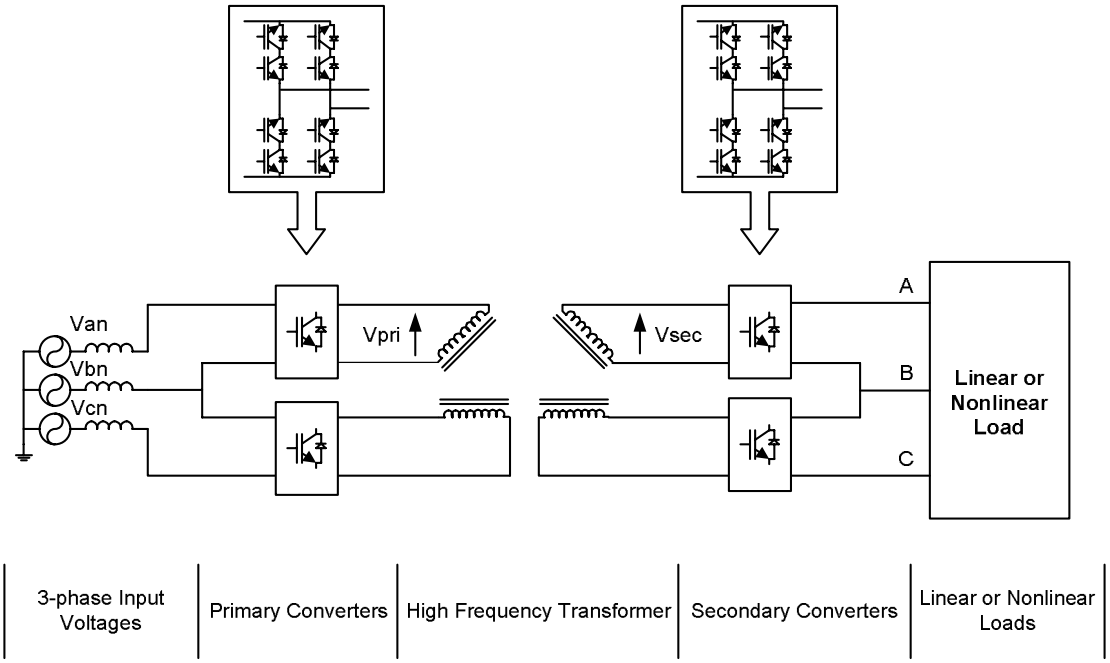

(b) Full-bridge open delta three-phase electronic transformer system.

Fig. 2.3. Topologies of three-phase electronic transformer system.

Number of semiconductor switches used in each topology of electronic transformer system is shown in Table 2.1.

Table 2.1. Number of semiconductor switches used in electronic transformer system.

Electronic Transformer System Topology	Number of switches
Half-bridge single phase electronic transformer system	8
Full-bridge single phase electronic transformer system	16
Half-bridge open delta three-phase electronic transformer system	16
Full-bridge open delta three-phase electronic transformer system	32

2.4.2 Analysis of electronic transformer

A. Single phase electronic transformer system

The single phase electronic transformer system shown in Fig. 2.2 (b) is analyzed mathematically as followed. Considering linear load condition, V_i is input voltage, and I_L is load current.

$$V_i = V_m \sin \omega_i t \tag{2.5}$$

$$I_L = I_m \sin\left(\omega_i t - \phi\right) \tag{2.6}$$

where V_m is peak input voltage.

I_m is peak load current.

ω_i is angular input frequency.

ϕ is power factor angle.

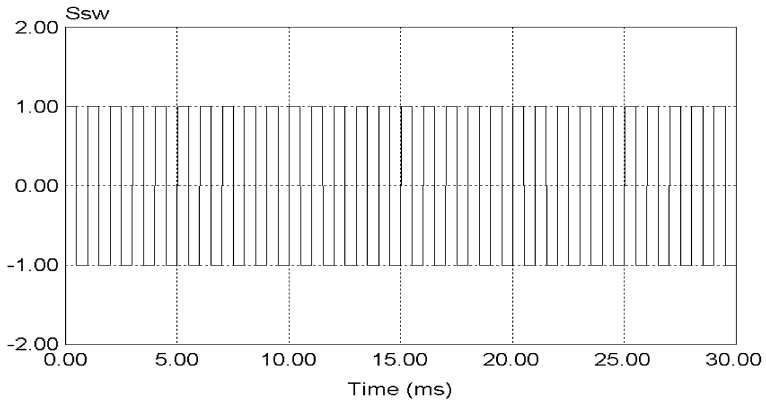

Fig. 2.4. Switching function for single phase electronic transformer system.

Switching function, S_{sw}, with 50% duty cycle as shown in Fig. 2.4. It is expressed in Fourier series with switching angular frequency of ω_s in (2.7).

$$S_{sw} = \sum_{n=odd}^{\infty} \frac{4}{n\pi} \sin(n\omega_s t) \tag{2.7}$$

The primary voltage of the transformer, V_{pri}, is the product of input voltage and the switching function as shown in (2.8). And the transformer primary winding current, I_{pri}, is the product of the load current and switching function as shown in (2.9).

$$V_{pri} = V_i \cdot S_{sw} = \frac{2V_m}{\pi} \sum_{n=odd}^{\infty} \frac{1}{n} \left[\cos(n\omega_s - \omega_i)t - \cos(n\omega_s + \omega_i)t \right] \tag{2.8}$$

$$I_{pri} = I_L \cdot S_{sw} = \frac{2I_m}{\pi} \sum_{n=odd}^{\infty} \frac{1}{n} \left[\cos\left((n\omega_s - \omega_i)t + \phi\right) - \cos\left((n\omega_s + \omega_i)t - \phi\right) \right] \tag{2.9}$$

Fig. 2.5 shows input voltage, transformer primary high frequency voltage, and output voltage of the single phase electronic transformer system in Fig. 2.2 (b).

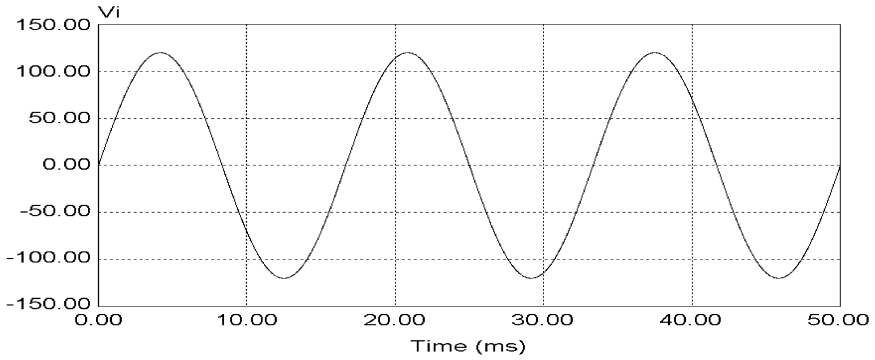

(a) Input voltage V_i (120 V 60 Hz).

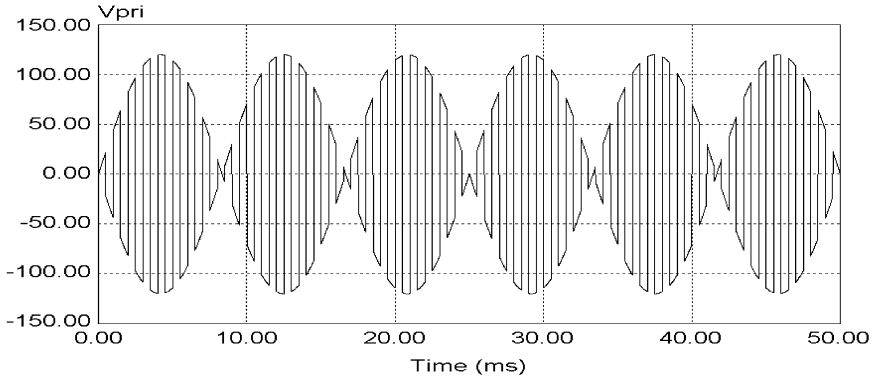

(b) Transformer primary voltage V_{pri} (1000 Hz).

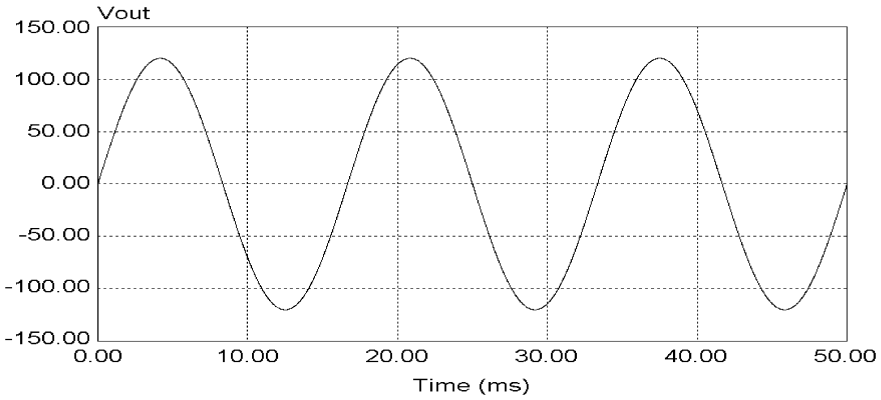

(c) Output voltage V_{out} (120 V 60 Hz).

Fig. 2.5. Single phase electronic transformer system voltages.

At nonlinear load condition, high frequency harmonic components of load current have effect to the current flowing through the transformer winding. Let the load current I_L be expressed in Fourier series as (2.10).

$$I_L = \sum_{h=1}^{\infty} A_h \sin\left(h\omega_i t\right) \tag{2.10}$$

The transformer winding current is:

$$I_{pri} = I_L \cdot S_{sw} = \frac{2}{\pi} \sum_{n=odd}^{\infty} \sum_{h=1}^{\infty} \frac{A_h}{n} \left[\cos\left(n\omega_s - h\omega_i\right)t - \cos\left(n\omega_s + h\omega_i\right)t \right] \tag{2.11}$$

Equation (2.11) shows undesirable DC component of transformer winding current when $n\omega_s = h\omega_i$, but it can be neglected if the switching frequency is much higher than the frequency of input voltage. Fig. 2.6 shows the currents of single phase electronic transformer system supplying nonlinear load.

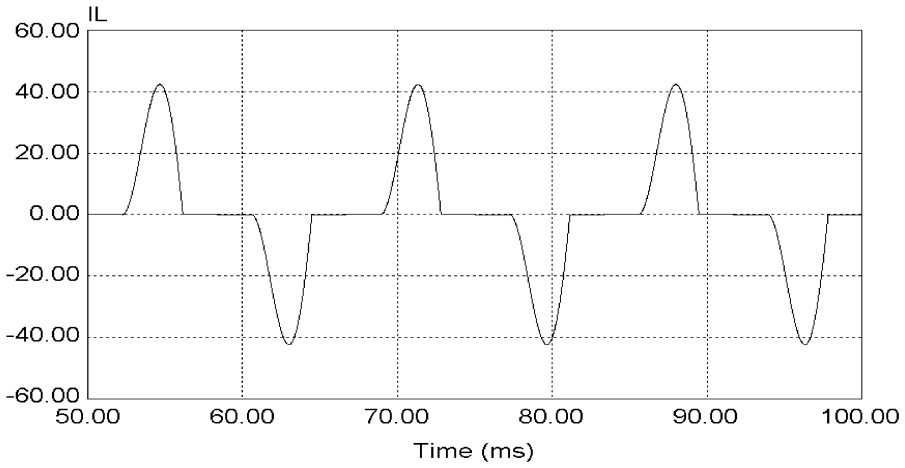

(a) Nonlinear load current.

Fig. 2.6. Single phase electronic transformer system currents.

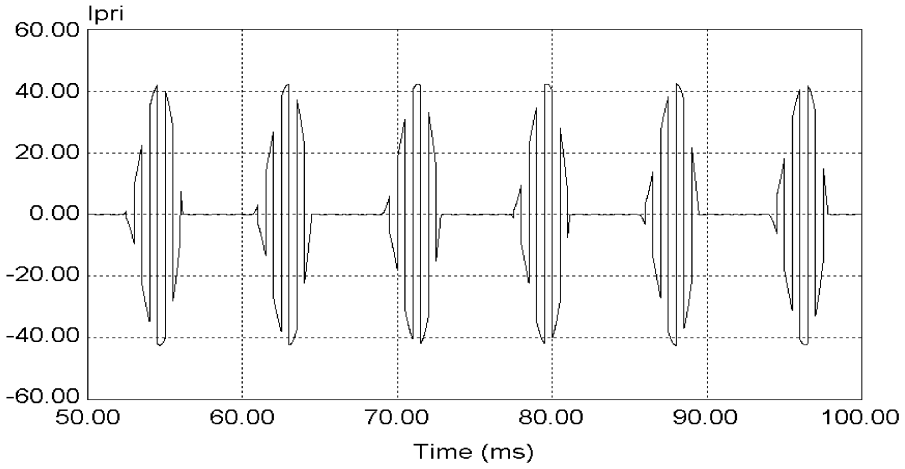

(b) Transformer primary current at nonlinear load condition.

Fig. 2.6. Continued.

B. Three-phase electronic transformer system

The analysis on the open delta three-phase electronic transformer system as shown in Fig. 2.3 is similar to the single phase system. Let V_{ab}, V_{bc}, and V_{ca} be input line voltages with peak voltage V_m, and input angular frequency of ω_i.

$$V_{ab} = V_m \sin(\omega_i t) \tag{2.12}$$

$$V_{bc} = V_m \sin\left(\omega_i t - \frac{2\pi}{3}\right) \tag{2.13}$$

$$V_{ca} = V_m \sin\left(\omega_i t + \frac{2\pi}{3}\right) \tag{2.14}$$

Switching function in (2.7) is applied to obtain transformer primary voltage as shown in (2.15). Equation (2.16) expresses output voltage V_{AB} of the open delta three-phase electronic transformer system.

$$V_{pri} = V_{ab} * S_{sw} \tag{2.15}$$

$$V_{AB} = V_{pri} * S_{sw} = V_{ab} \tag{2.16}$$

Fig. 2.7 shows three-phase input line voltages and primary high frequency voltage of the open delta three-phase electronic transformer system.

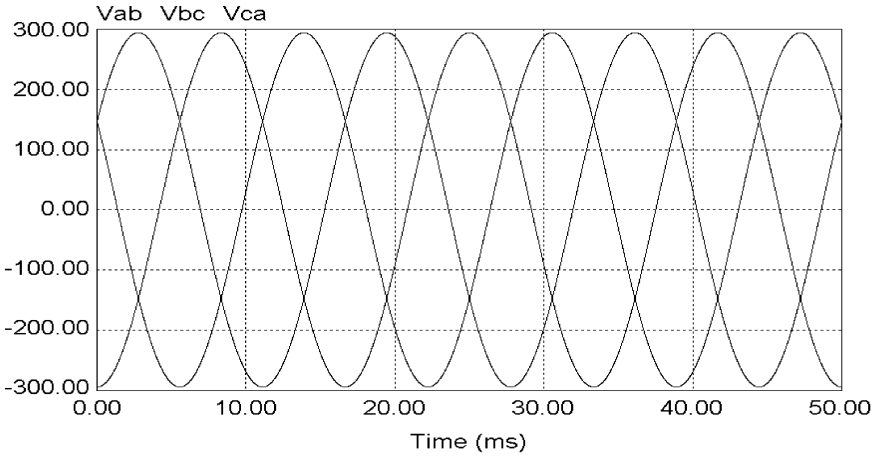

(a) Three-phase input line voltages (208 V 60 Hz).

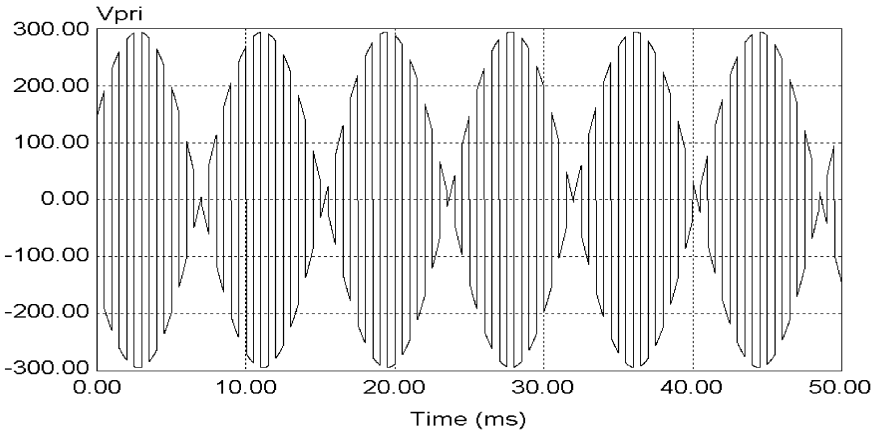

(b) Primary voltage of the transformer (1000 Hz).

Fig. 2.7. Three-phase electronic transformer system voltages.

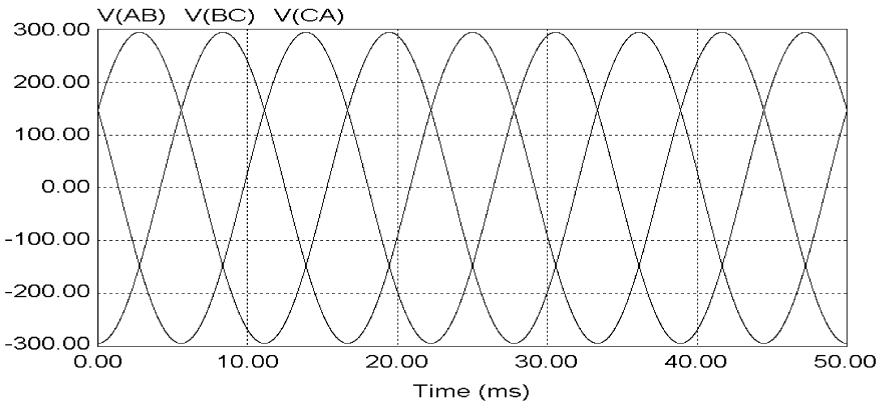

(c) Transformer sinusoidal output voltages (208 V 60 Hz).

Fig. 2.7. Continued.

2.4.3 4-step switching strategy

Electronic transformer has difficulties to commutate inductive load current from one bi-directional switch to another due to finite switch on/off time [1]. Since the on/off operation of semiconductor switch requires delay time, an overlap between switching may cause short-circuited to the source input voltage and results in interrupting inductive load current. Hence, snubber circuits are required on input and output sides. To control each semiconductor switch of any bi-directional switch independently, 4-step switching strategy is applied. The approach depends on polarity of input voltage or load current.

With an inductive load, switching operation can be divided into 4 modes according to the polarity of input voltage and load current as following [1], [12].

Mode 1 : $V_i > 0$; $I_L > 0$

Mode 2 : $V_i > 0$; $I_L < 0$

Mode 3 : $V_i < 0$; $I_L > 0$

Mode 4 : $V_i < 0$; $I_L < 0$

The operation of 4-step switching sequence is divided into voltage and current reference mode according to the reference signal.

A. Voltage reference mode

Voltage reference mode uses input voltage polarity as the reference signal. Therefore, switching sequences of operation mode 1 and 2 are the same, and switching sequences of operation mode 3 and 4 are also the same.

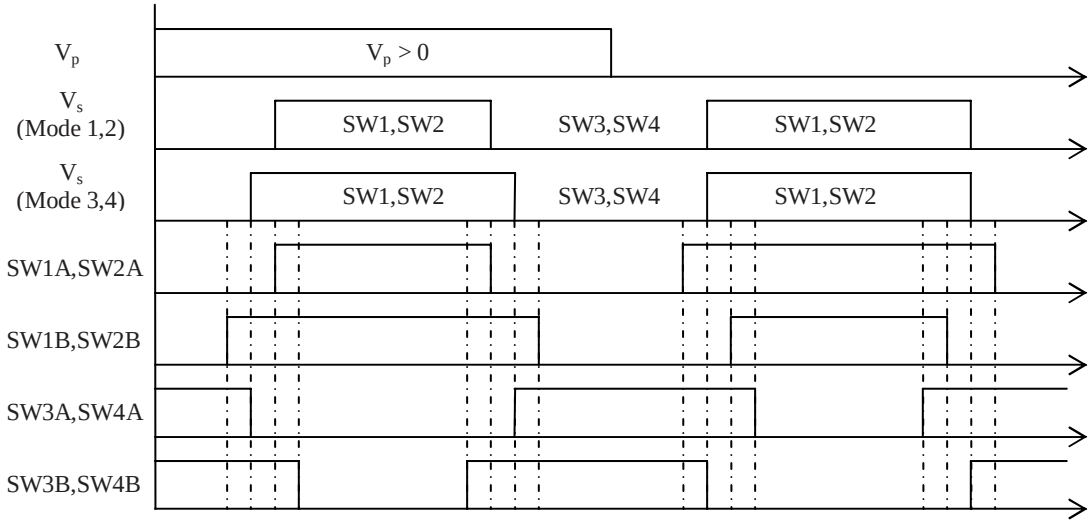

Fig. 2.8. Example of gate signals by 4-step switching voltage reference mode.

Table 2.2. Voltage reference 4-step switching sequence.

(a) Positive reference signal

	INIT	Step 1	Step 2	Step 3	Step 4
SW1A SW2A	ON	ON	OFF	OFF	OFF
SW1B SW2B	ON	ON	ON	ON	OFF
SW3A SW4A	OFF	OFF	OFF	ON	ON
SW3B SW4B	OFF	ON	ON	ON	ON
Mode 1	No Change	No Change	Switching	No Change	No Change
Mode 2	No Change	No Change	No Change	Switching	No Change

(b) Negative reference signal

	INIT	Step 1	Step 2	Step 3	Step 4
SW1A SW2A	ON	ON	ON	ON	OFF
SW1B SW2B	ON	ON	OFF	OFF	OFF
SW3A SW4A	OFF	ON	ON	ON	ON
SW3B SW4B	OFF	OFF	OFF	ON	ON
Mode 1	No Change	No Change	Switching	No Change	No Change
Mode 2	No Change	No Change	Switching	No Change	No Change

Table 2.2 shows the switch operation sequences of commutation from switches SW1, SW2 to SW3, SW4 based on Fig. 2.2 (b). In case of commutation from SW3, SW4 to SW1, SW2, the operation sequence is reversed. The example of gate signals in voltage reference mode is shown in Fig. 2.8 where V_p represents input voltage polarity as reference signal, and V_s represents switch conduction state [1].

B. Current reference mode

Current reference mode uses load current polarity as a reference signal. Therefore, switching sequences of operation mode 1 and 3 are the same, and switching sequences of operation mode 2 and 4 are also the same. The example of gate signals in current reference mode is shown in Fig. 2.9 where V_p represents load current polarity as reference signal, and V_s represents switch conduction state.

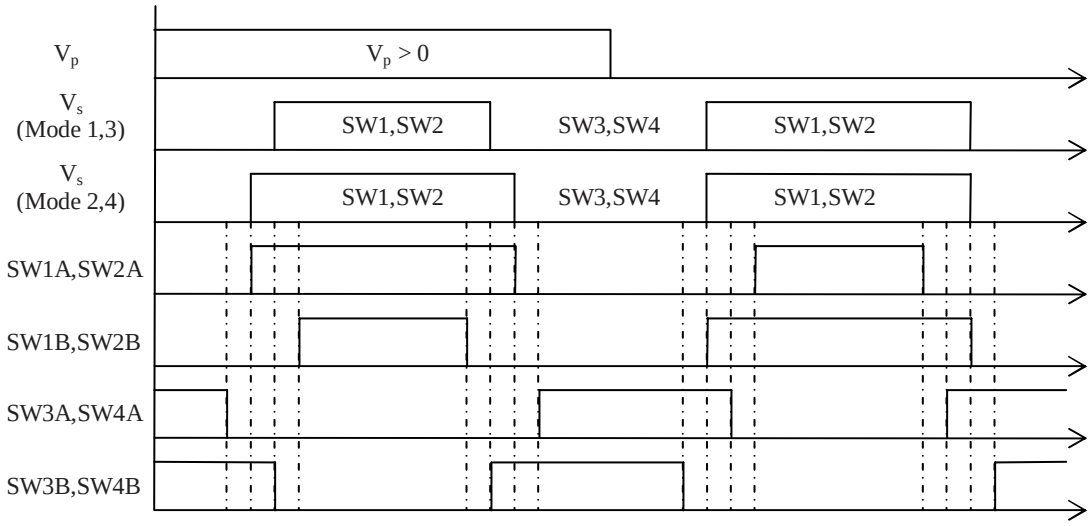

Fig. 2.9. Example of gate signals by 4-step switching current reference mode.

Table 2.3 shows the switch operation sequences of commutation from switches SW1, SW2 to SW3, SW4. Similarly to the voltage reference mode, commutation from SW3, SW4 to SW1, SW2, the operation sequence is reversed.

Table 2.3. Current reference 4-step switching sequence.

(a) Positive reference signal

	INIT	Step 1	Step 2	Step 3	Step 4
SW1A SW2A	ON	ON	ON	OFF	OFF
SW1B SW2B	ON	OFF	OFF	OFF	OFF
SW3A SW4A	OFF	OFF	OFF	OFF	ON
SW3B SW4B	OFF	OFF	ON	ON	ON
Mode 1	No Change	No Change	No Change	Switching	No Change
Mode 2	No Change	No Change	Switching	No Change	No Change

(b) Negative reference signal

	INIT	Step 1	Step 2	Step 3	Step 4
SW1A SW2A	ON	OFF	OFF	OFF	OFF
SW1B SW2B	ON	ON	ON	OFF	OFF
SW3A SW4A	OFF	OFF	ON	ON	ON
SW3B SW4B	OFF	OFF	OFF	OFF	ON
Mode 1	No Change	No Change	Switching	No Change	No Change
Mode 2	No Change	No Change	No Change	Switching	No Change

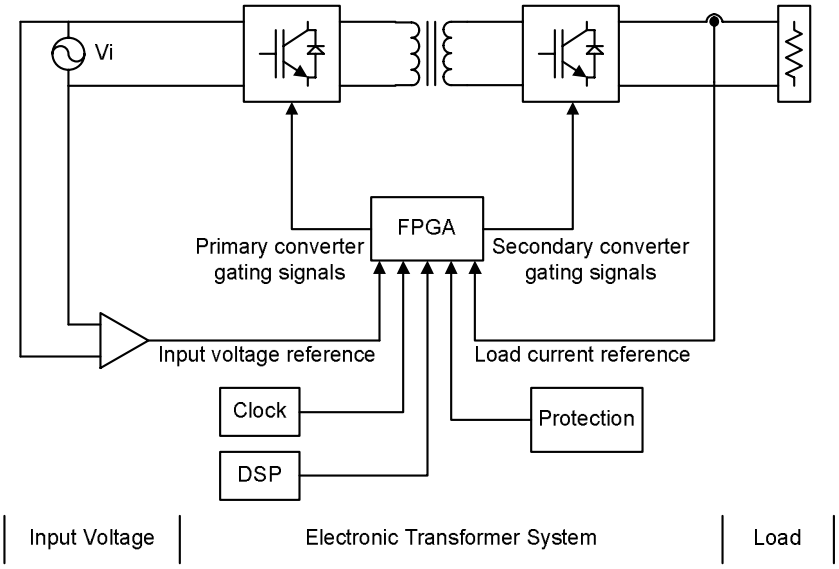

Fig. 2.10. Block diagram of gating signal selection through FPGA.

To apply the 4-step switching technique to the converters in electronic transformer system, the reference mode is considered. To ease the complexity, the primary converter should be operated with voltage reference mode, and the secondary converter with current reference mode. The sequences of converter switch gate signals are achieved through the Field-Programmable Gate Array (FPGA), which is an EEPROM based programmable logic device as shown in Fig. 2.10.

2.5 Electronic transformer applications in power distribution system

In power distribution system, transformers are fundamental components. They are rather inexpensive, highly reliable and relatively efficient. They are employed to enable electric generating stations to supply power to the electric grid, and also enable plants to have access to an off-site power source for start up. However, the

transformers possess some undesirable properties including sensitivity to harmonics, voltage drop under load, required protection from the system disruptions and overload, protection of the system from problems arising at or beyond the transformer, environmental concerns regarding mineral oil and performance under DC-offset load unbalances. These disadvantages are becoming increasingly important as power quality becomes more of a concern. Electronic transformer is based on power electronic, which offers following advantages over conventional transformer [13].

- Protect power distribution system and user from harmonics propagation.
- Able to perform input power factor correction.
- Zero regulation available.
- Prevents faults from affecting the power distribution system.
- Able to supply load with DC offsets.
- Not utilize mineral oil or liquid dielectric which is environmental friendly.

A concept of single phase electronic distribution transformer is proposed in [14]. It is shown to improve power quality under critical load condition. The proper AC/AC converter design and turn ratio of the transformer provide ride-through capability during disturbances while regulating the output voltage. It also restores the sinusoidal voltage when the utility voltage is distorted due to nonlinear load condition. The transformer can be utilized in low-voltage distribution (480 V/120 V). The single phase distribution transformer is shown in Fig. 2.11.

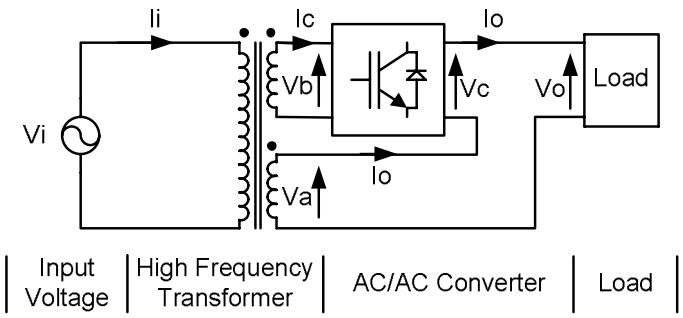

Fig. 2.11. Single phase distribution transformer.

$$V_o = V_a + V_c \tag{2.17}$$

$$V_o = a * V_i + b * D * V_i \tag{2.18}$$

where a and b are turn ratios of each winding.

D is duty cycle of the converter.

Under normal condition, V_i = 1 per-unit, a = 0.6667 and b = 1.3333. Then

$$V_a = 0.6667 \text{ per-unit} \tag{2.19}$$

$$V_b = 1.3333 \text{ per-unit} \tag{2.20}$$

Duty cycle, D, is selected to be 0.25 to yield V_c = 0.3333 per-unit. Output voltage is

$$V_o = V_a + V_c = 1 \text{ per-unit} \tag{2.21}$$

Under 50% sag condition, V_a = 0.3333 per-unit and V_b = 0.6667 per-unit. Duty cycle is selected to be 1 to yield V_c = 0.6667 per-unit and maintain output voltage at 1 per-unit.

2.6 Conclusion

In this chapter, concept of electronic transformer system has been presented. Operation of a transformer at high frequency has been discussed. Topologies of electronic transformer system employing primary and secondary converters were described and analyzed. The 4-step switching strategy allows safe commutation without snubber circuits, which losses can be reduced. Advantages of applying electronic transformer to the power distribution system have been explained. Application on electronic transformer as distribution transformer has been described.

CHAPTER III

AUTO-CONNECTED ELECTRONIC PHASE-SHIFTING TRANSFORMER IN ELECTRICAL DISTRIBUTION SYSTEM

3.1 Introduction

Presently, the uses of modern power electronic equipments are increasing continually in industry. The power electronic equipments employing three-phase diode rectifier type utility interface include switch mode power supply, and adjustable speed drive system (ASDs), which are categorized as nonlinear loads. The nonlinear loads generate harmonics of order 6k±1, which is 5, 7, 11, 13, etc., in utility line currents of the electric power distribution system. The IEEE 519 and IEC 61000-3-4 are standards that set the limits in order to reduce negative effects of the harmonics.

Many approaches to control and reduce the harmonics have been studied and published. Previously, the harmonic reduction was done by applying multi-pulse transformers. It is well known that certain harmonics can be cancelled with the proper phase-shifting angle on the secondary side of the transformers [6]. The concept is that the harmonics generated by one converter are cancelled with harmonics generated by other converter. For example, with wye connection and a delta connection yields a 30° phase-shifting angle, and 5^{th} and 7^{th} harmonics can be eliminated and the current THD is improved. This technique is found to be excessive bulky and inefficient [15]. References [6], [16]-[19] outline a variety of line frequency phase-shifting transformer

connections to reduce harmonics generated by nonlinear loads in electric power distribution system. However, these transformers suffer from large size, weight and occupy large floor space.

Later, the concept of polyphase autotransformer, as shown in Fig. 3.1, was introduced [3], [6]. Instead of conventional wye/delta/wye isolation transformer as mentioned, it provides the appropriated phase-shifting angle through the auto connection. With this concept, the VA rating of magnetic components can be greatly reduced. The phase-shifting angle of the rectifier input voltages for each load is selected such that 5^{th} and 7^{th} harmonics are cancelled in the input line current.

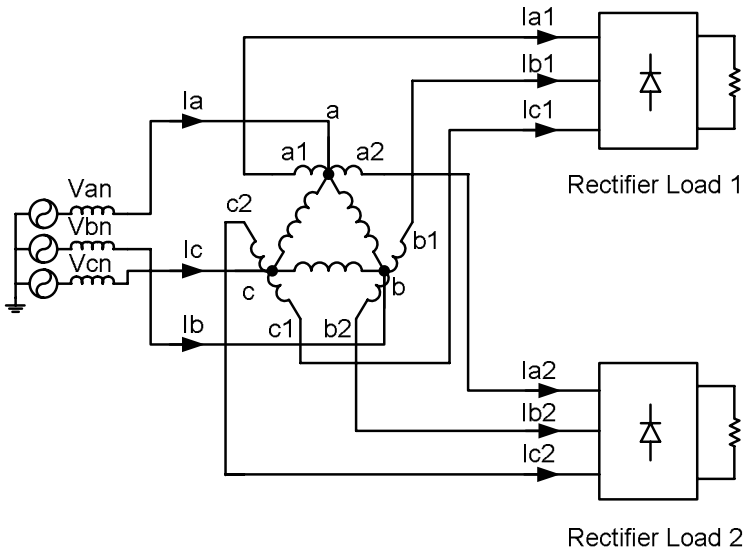

Fig. 3.1. Circuit diagram of the polyphase autotransformer.

In view of this, the research proposes an auto-connected electronic phase-shifting transformer. The objective of the proposed approach is to reduce size and weight of the phase-shifting transformer used in harmonic current reduction. The proposed approach employs power electronic AC/AC frequency converters on both primary and secondary sides of the transformers in order to operate the core at high frequency, and retrieve the voltages at the line frequency for the loads. The AC/AC converters permit bi-directional power flow. A unique 4-step switching strategy is employed to realize snubber-less operation of the AC/AC converter. Further, bulky input and output filters are absent in the proposed approach. The input and output function of the proposed electronics transformer is identical to its line frequency counterpart. A phase-shifting angle of 30° is achieved and 5^{th} and 7th harmonics generated by nonlinear loads are subtracted. The overall utility input total harmonic distortion (THD) is shown to be improved.

The advantages of the proposed approach are:

- No DC-link capacitor required.
- Size reduction of transformer since it operates at high frequency.
- Reduce number of solid-state IGBT switches required.
- Low kVA rating (0.18 per-unit).
- Snubber-less operation without input and output filters.

3.2 Proposed topology

In Fig. 3.2, the proposed auto-connected electronic phase-shifting transformer to cancel harmonics generated by rectifier type nonlinear loads is shown. The AC/AC power electronic converters are presented with auto-connected phase-shifting transformers. In electrical power distribution system, three-phase voltages are supplied through half-bridge frequency converters, which operate with high switching frequency, to obtain high frequency voltages for the electronic phase-shifting transformers. Bi-directional switches are employed in the converters to maintain bi-directional power flow.

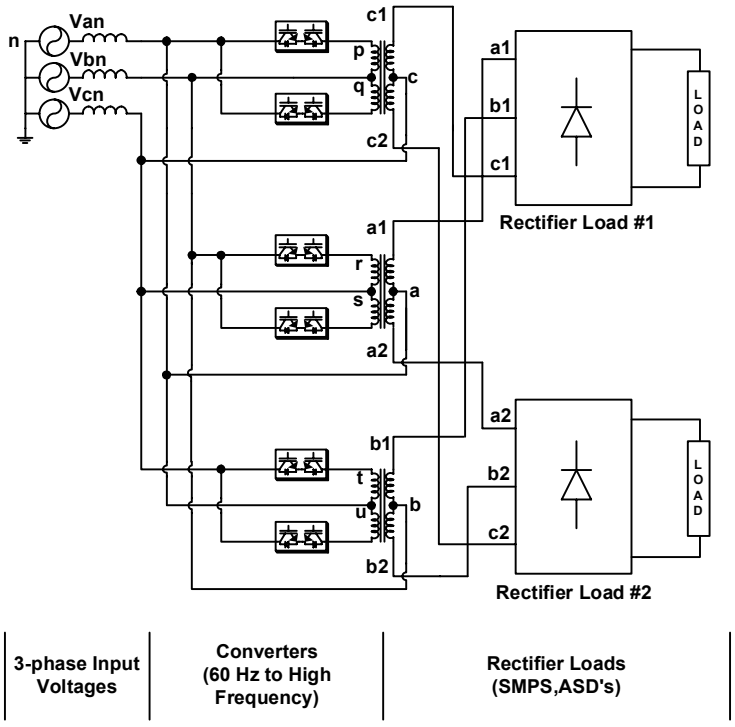

Fig. 3.2. Proposed auto-connected electronic transformer for cancelling 5^{th} and 7^{th} harmonics generated in rectifier loads.

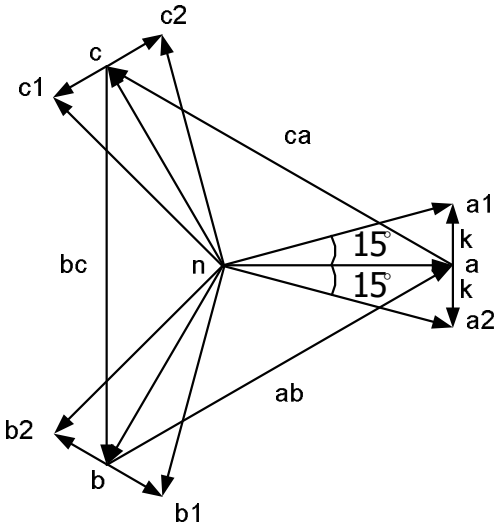

Fig. 3.3. Vector diagram of phase-shifting autotransformer.

The winding length of the transformer can be set to achieve cancellation of certain harmonics. To eliminate 5th and 7th harmonics in the input line currents, the phase-shifting angle is selected to be 30°. From the vector diagram in Fig. 3.3, the angle between vector $\boldsymbol{a_1n}$ and vector $\boldsymbol{an}$ is 15°, which is the same as, the angle between vector $\boldsymbol{a_2n}$ and vector $\boldsymbol{an}$. The required winding length is found by

$$k = \frac{\tan(15^\circ)}{\sqrt{3}} = 0.1547 \tag{3.1}$$

The voltages induced to the secondary side of the transformer, which contains high frequency components, are supplied to the loads. The 30° phase-shifting angle is achieved by the auto-connection of the transformers.

Due to the 30° phase-shifting angle, each identical nonlinear load generates 5th and 7th harmonics, which have the same magnitude, but opposite in direction.

Therefore, the 5^{th} and 7^{th} harmonics generated by each nonlinear load can cancel each other in the input line currents.

Fig. 3.4 shows a variation of the topology shown in Fig. 3.2. The topology in Fig. 3.4 is more suitable for a combination of linear and nonlinear loads. Additional AC/AC converters are attached on secondary side of the transformer in order to produce sinusoidal voltage waveforms at the utility frequency. The voltages applied to the loads do not contain any high frequency components. The same results on harmonic cancellation in the input line currents can be achieved.

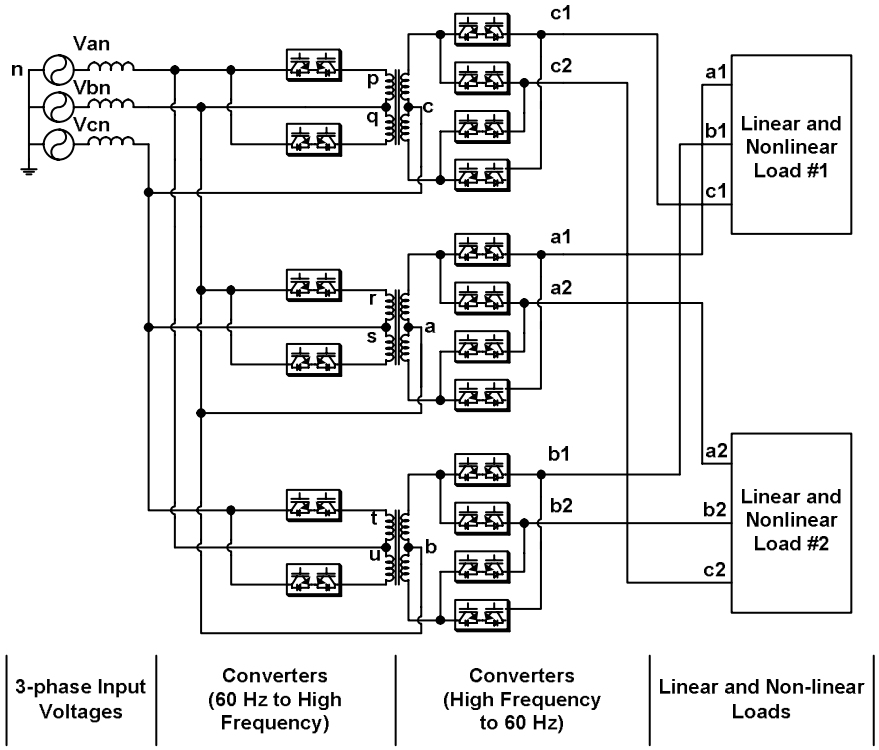

Fig. 3.4. The alternative auto-connected electronics phase-shifting transformer topology.

3.3 Analysis of the proposed topology

In this section, the analysis of output voltages and input currents of the topology are presented.

3.3.1 Voltage analysis

Let the three-phase input phase voltages with angular frequency of ω_i be,

$$V_{an} = V_m \sin \omega_i t \tag{3.2}$$

$$V_{bn} = V_m \sin\left(\omega_i t - \frac{2\pi}{3}\right) \tag{3.3}$$

$$V_{cn} = V_m \sin\left(\omega_i t + \frac{2\pi}{3}\right) \tag{3.4}$$

From the approach topology in Fig. 3.2, the modulated high frequency line voltages from the converter, which are applied to primary winding of the transformer, are:

$$V_{pq} = V_{ab} \cdot S_{sw} \tag{3.5}$$

$$V_{rs} = V_{bc} \cdot S_{sw} \tag{3.6}$$

$$V_{tu} = V_{ca} \cdot S_{sw} \tag{3.7}$$

where S_{sw} is switching function of the converter with angular switching frequency ω_s.

$$S_{sw} = \sum_{n=odd}^{\infty} \frac{4}{n\pi} \sin\left(n\omega_s t\right) \tag{3.8}$$

From the phase-shifting auto-transformer connection, as shown in the vector diagram in Fig. 3.3,

$$v_{a_1a} = -V_{rs} \cdot k \tag{3.9}$$

$$v_{b_1b} = -V_{tu} \cdot k \tag{3.10}$$

$$v_{c_1c} = -V_{pq} \cdot k \tag{3.11}$$

$$v_{a_2a} = V_{rs} \cdot k \tag{3.12}$$

$$v_{b_2b} = V_{tu} \cdot k \tag{3.13}$$

$$v_{c_2c} = V_{pq} \cdot k \tag{3.14}$$

Equations (3.5) - (3.11) yield the voltages to the rectifier load #1,

$$v_{a_1n} = V_{an} + V_{a_1a} = V_{an} - k \cdot V_{bc} \cdot S_{sw} \tag{3.15}$$

$$v_{b_1n} = V_{bn} + V_{b_1b} = V_{bn} - k \cdot V_{ca} \cdot S_{sw} \tag{3.16}$$

$$v_{c_1n} = V_{cn} + V_{c_1c} = V_{cn} - k \cdot V_{ab} \cdot S_{sw} \tag{3.17}$$

Equations (3.5) - (3.7) and (3.12) - (3.14) yield the voltages to the rectifier load #2,

$$v_{a_2n} = V_{an} + V_{a_2a} = V_{an} + k \cdot V_{bc} \cdot S_{sw} \tag{3.18}$$

$$v_{b_2n} = V_{bn} + V_{b_2b} = V_{bn} + k \cdot V_{ca} \cdot S_{sw} \tag{3.19}$$

$$v_{c_2n} = V_{cn} + V_{c_2c} = V_{cn} + k \cdot V_{ab} \cdot S_{sw} \tag{3.20}$$

3.3.2 Current analysis

A. Balanced nonlinear load

The rectifier type nonlinear loads are assumed to be highly inductive loads. Due to the high frequency components in rectifier input voltages, the currents at the rectifier input of nonlinear load #1 in Fig. 3.2 can be expressed as:

$$I_{a_1} = I_{o_1}\left[S_{ax}(\omega t) + 0.5\{1+S_{sw}(\omega_s t)\}S_{ay}(\omega t) + 0.5\{1-S_{sw}(\omega_s t)\}S_{az}(\omega t)\right] \quad (3.21)$$

$$I_{b_1} = I_{o_1}\left[S_{ax}\left(\omega t-\frac{2\pi}{3}\right) + 0.5\{1+S_{sw}(\omega_s t)\}S_{ay}\left(\omega t-\frac{2\pi}{3}\right) + 0.5\{1-S_{sw}(\omega_s t)\}S_{az}\left(\omega t-\frac{2\pi}{3}\right)\right] \quad (3.22)$$

$$I_{c_1} = I_{o_1}\left[S_{ax}\left(\omega t+\frac{2\pi}{3}\right) + 0.5\{1+S_{sw}(\omega_s t)\}S_{ay}\left(\omega t+\frac{2\pi}{3}\right) + 0.5\{1-S_{sw}(\omega_s t)\}S_{az}\left(\omega t+\frac{2\pi}{3}\right)\right] \quad (3.23)$$

where $S_{ax}(\omega t) = \sum_{n=odd}^{\infty}\frac{4}{n\pi}\cos\left(\frac{n\pi}{4}\right)\sin(n\omega t)$

$$S_{ay}(\omega t) = \sum_{n=odd}^{\infty}\frac{4}{n\pi}\cos\left(\frac{5n\pi}{12}\right)\sin\left(n\left(\omega t-\frac{\pi}{3}\right)\right)$$

$$S_{az}(\omega t) = \sum_{n=odd}^{\infty}\frac{4}{n\pi}\cos\left(\frac{5n\pi}{12}\right)\sin\left(n\left(\omega t+\frac{\pi}{3}\right)\right)$$

For nonlinear load #2,

$$I_{a_2} = I_{o_2}\left[S_{ax}(\omega t) + 0.5\{1-S_{sw}(\omega_s t)\}S_{ay}(\omega t) + 0.5\{1+S_{sw}(\omega_s t)\}S_{az}(\omega t)\right] \quad (3.24)$$

$$I_{b_2} = I_{o_2}\left[S_{ax}\left(\omega t-\frac{2\pi}{3}\right) + 0.5\{1-S_{sw}(\omega_s t)\}S_{ay}\left(\omega t-\frac{2\pi}{3}\right) + 0.5\{1+S_{sw}(\omega_s t)\}S_{az}\left(\omega t-\frac{2\pi}{3}\right)\right] \quad (3.25)$$

$$I_{c_2} = I_{o_2}\left[S_{ax}\left(\omega t+\frac{2\pi}{3}\right) + 0.5\{1-S_{sw}(\omega_s t)\}S_{ay}\left(\omega t+\frac{2\pi}{3}\right) + 0.5\{1+S_{sw}(\omega_s t)\}S_{az}\left(\omega t+\frac{2\pi}{3}\right)\right] \quad (3.26)$$

where I_{o_1} and I_{o_2} are DC output currents of nonlinear load #1 and #2 , respectively.

The utility input currents can be expressed as:

$$I_a = I_{a_1} + I_{a_2} + I_{pq} - I_{tu} \tag{3.27}$$

$$I_b = I_{b_1} + I_{b_2} + I_{rs} - I_{pq} \tag{3.28}$$

$$I_c = I_{c_1} + I_{c_2} + I_{tu} - I_{rs} \tag{3.29}$$

where $I_{pq} = k \cdot \left(I_{c_2} - I_{c_1} \right)$, $I_{rs} = k \cdot \left(I_{a_2} - I_{a1} \right)$, and $I_{tu} = k \cdot \left(I_{b_2} - I_{b1} \right)$.

Equations (3.27), (3.28), and (3.29) can be expressed as:

$$I_a = I_{a_1} + I_{a_2} + k\left(I_{c_2} - I_{c_1} - I_{b_2} + I_{b_1} \right) \tag{3.30}$$

$$I_b = I_{b_1} + I_{b_2} + k\left(I_{a_2} - I_{a_1} - I_{c_2} + I_{c_1} \right) \tag{3.31}$$

$$I_c = I_{c_1} + I_{c_2} + k\left(I_{b_2} - I_{b_1} - I_{a_2} + I_{a_1} \right) \tag{3.32}$$

In the balanced loads condition, $I_{o_1} = I_{o_2} = I_o$. The utility line current of phase A (I_a) can be expressed as:

$$I_a = I_o\left[2S_{ax}(\omega t) + S_{ay}(\omega t) + S_{az}(\omega t) + k\left\{ S_{az}\left(\omega t + \frac{2\pi}{3} \right) - S_{ay}\left(\omega t + \frac{2\pi}{3} \right) - S_{az}\left(\omega t - \frac{2\pi}{3} \right) + S_{ay}\left(\omega t - \frac{2\pi}{3} \right) \right\} \right] \tag{3.33}$$

Equation (3.33) shows that 5th and 7th harmonics are eliminated when proper value of k is selected.

B. Unbalanced nonlinear load

At unbalanced loads condition of the topology in Fig. 3.2, the utility line current is affected by high frequency components generated through switching frequency of the converter. At lower switching frequency, i.e. 1-5 kHz, the utility line

current contains some sub-harmonics, which affect the quality of input line current. From (3.8) and (3.30) – (3.32), the expected orders h are:

$$h = n_i\omega_i \pm n_s\omega_s \tag{3.34}$$

where n_i and n_s are harmonic orders generated by input frequency and switching frequency, respectively.

Under unbalance loads condition, the utility line current of phase A ($I_a^{'}$) can be expressed as:

$$I_a^{'} = I_a + I_{a,h} \tag{3.35}$$

$$I_{a,h} = C_h * \left(\cos\left(\left(n_i\omega_i - n_s\omega_s\right)t\right) - \cos\left(\left(n_i\omega_i + n_s\omega_s\right)t\right)\right) \tag{3.36}$$

$$C_h = \left(\frac{4}{n_s\pi}\right) * \left(\frac{I_{o_2} - I_{o_1}}{4}\right) * \left\{\sqrt{3} * k * \left(\frac{4}{n_i\pi}\right) * \left[2\cos\left(\frac{4}{n_i\pi}\right) + \left(\frac{5n_i\pi}{12}\right) * \left(1 + 2\cos\left(\frac{n_i\pi}{3}\right)\right)\right]\right\} \tag{3.37}$$

where I_a is defined in (3.33).

The 5th and 7th harmonics in utility line currents are very small, which can be neglected, but the sub-harmonics as shown in (3.36) cause total harmonic distortion (THD) to be higher. The effect of sub-harmonics maybe reduced with higher switching frequency.

At unbalanced loads condition of the topology in Fig. 3.4, different utility current analysis is presented due to the absence of high frequency components in rectifier load type input voltage. The input currents of nonlinear load #1 can be expressed as:

$$I_{a_1} = \sum_{n=odd}^{\infty} \frac{4 * I_{o_1}}{n\pi} \sin\left(n\left(\omega t + \frac{\pi}{12} \right) \right) \tag{3.38}$$

$$I_{b_1} = \sum_{n=odd}^{\infty} \frac{4 * I_{o_1}}{n\pi} \sin\left(n\left(\omega t - \frac{7\pi}{12} \right) \right) \tag{3.39}$$

$$I_{c_1} = \sum_{n=odd}^{\infty} \frac{4 * I_{o_1}}{n\pi} \sin\left(n\left(\omega t + \frac{3\pi}{4} \right) \right) \tag{3.40}$$

For nonlinear load #2, the input currents can be expressed as:

$$I_{a_2} = \sum_{n=odd}^{\infty} \frac{4 * I_{o_2}}{n\pi} \sin\left(n\left(\omega t - \frac{\pi}{12} \right) \right) \tag{3.41}$$

$$I_{b_2} = \sum_{n=odd}^{\infty} \frac{4 * I_{o_2}}{n\pi} \sin\left(n\left(\omega t - \frac{3\pi}{4} \right) \right) \tag{3.42}$$

$$I_{c_2} = \sum_{n=odd}^{\infty} \frac{4 * I_{o_2}}{n\pi} \sin\left(n\left(\omega t + \frac{7\pi}{12} \right) \right) \tag{3.43}$$

From (3.30), the harmonic components of utility current of phase A, $I_{a,n}$, can be expressed in (3.44).

At n = 5, 7, 11, 13, 17, 19 …

$$\begin{aligned} I_{a,n} = \frac{4}{n\pi} \Bigg[& \left(I_{o_1} + I_{o_2} \right) \left(\cos\left(\frac{n\pi}{12} \right) + 2 * k * \sin\left(\frac{2n\pi}{3} \right) * \sin\left(\frac{n\pi}{12} \right) \right) \sin\left(n\omega t \right) \\ & + \left(I_{o_1} - I_{o_2} \right) \left(\sin\left(\frac{n\pi}{12} \right) - 2 * k * \sin\left(\frac{2n\pi}{3} \right) * \cos\left(\frac{n\pi}{12} \right) \right) \cos\left(n\omega t \right) \Bigg] \end{aligned} \tag{3.44}$$

where k is the selected transformer winding length.

Equations (3.44) shows that 5^{th} and 7^{th} harmonics are not cancelled due to the difference of loads $\left(I_{o_1} - I_{o_2}\right)$. Thus, the total harmonic distortion (THD) is increased according to the unbalance of nonlinear loads.

Let $\left(I_{o_1} + I_{o_2}\right)$ be 1 per-unit, and the total harmonic distortion (THD) of input current at balanced load is 1 per-unit. The increase of unbalance loads causes higher THD as shown in Fig. 3.5.

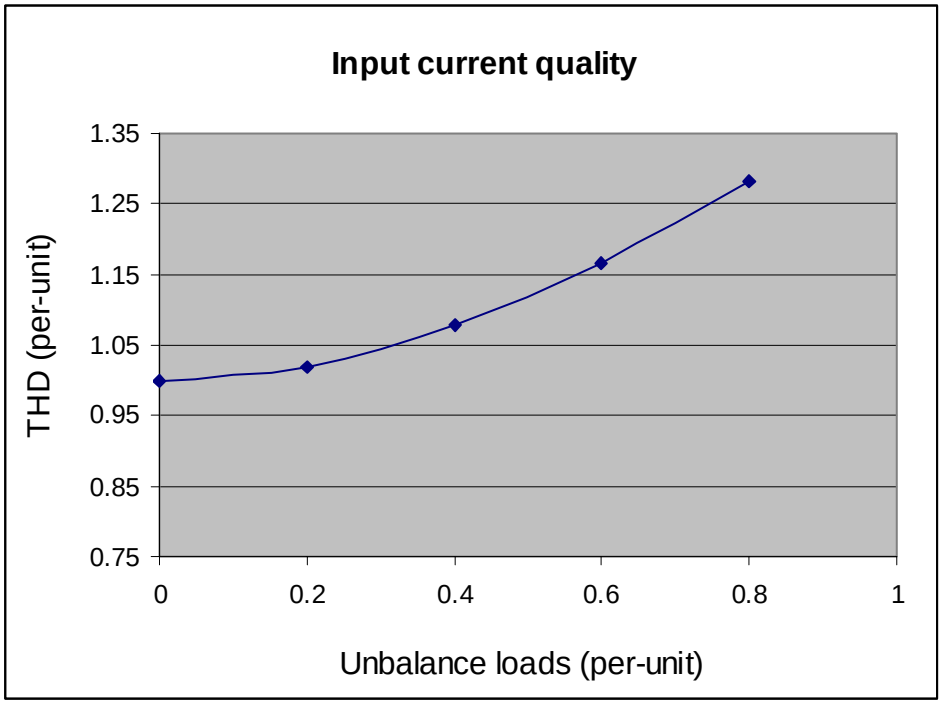

Fig. 3.5. Utility line current THD in per-unit at unbalanced loads.

3.4 Design example

The system of input voltage 208 V, 10 kVA is considered. The switching frequency is assumed to be 1000 Hz. The VA rating of the system is summarized in Table 3.1, where P_o is the output power. The 5^{th} and 7^{th} harmonic cancellation of rectifier load #1 and #2 are equal.

Table 3.1. VA rating of the system.

	VA rating of auto-connected transformer (per-unit)	VA rating of static converter (per-unit)	Number of IGBTs
Approach in Fig. Fig. 3.2	$0.18\,P_o$	$0.061\,P_o$	12
Approach in Fig. Fig. 3.4	$0.18\,P_o$	$0.061\,P_o$	36

3.5 Simulation results

The proposed approach, as shown in Fig. 3.2, was simulated with input voltage of 208 V at 60 Hz, as shown in Fig. 3.6. The switching frequency of the converters was set at 1000 Hz to operate the phase-shifting transformer at high frequency. The high frequency voltages of the transformer are shown in Fig. 3.7. Also, the spectrums of the high frequency voltages of the transformer are shown in Fig. 3.8.

The phase-shifting voltages are achieved with the auto-connection of the transformer. Fig. 3.9 shows the voltages supplied to a nonlinear load, which contains

high frequency components, with +15° phase-shifted and another one with -15° phase-shifted.

Diode rectifiers were simulated as the nonlinear loads. The input currents of the rectifiers and their spectrums are shown in Fig. 3.10 and Fig. 3.11. The 5^{th} and 7^{th} harmonics of the rectifier currents exist. The line input currents and their spectrums are shown in Fig. 3.12 and Fig. 3.13. The 5^{th} and 7^{th} harmonics are cancelled in the electronic transformer as they are absented.

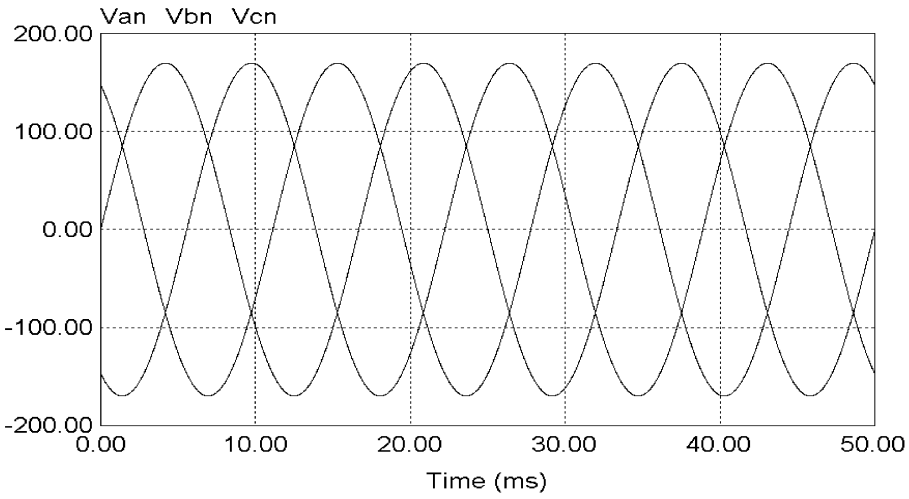

Fig. 3.6. Input line-to-neutral voltages, V_{an}, V_{bn}, and V_{cn} at 60 Hz.

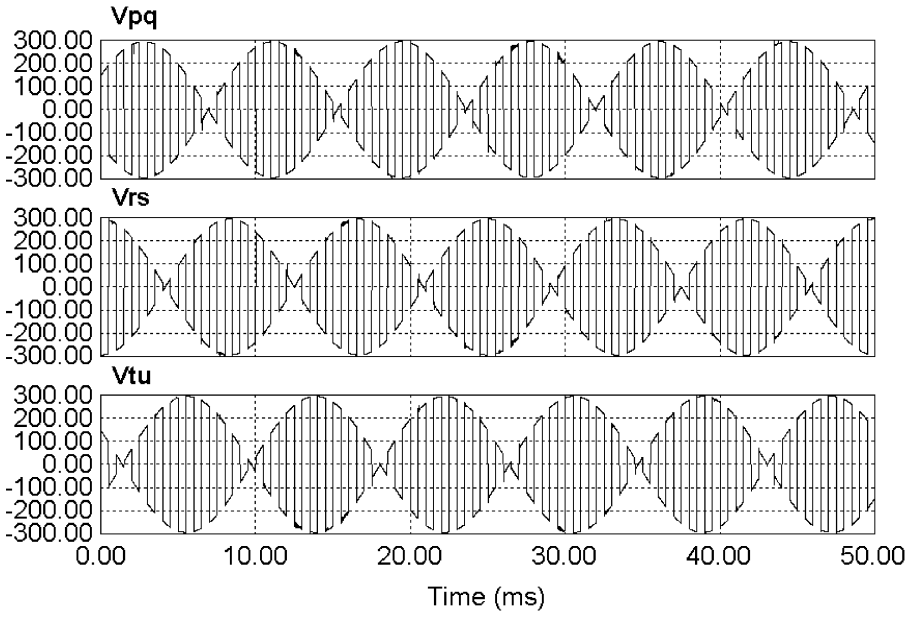

Fig. 3.7. High frequency voltages on the transformer primary side.

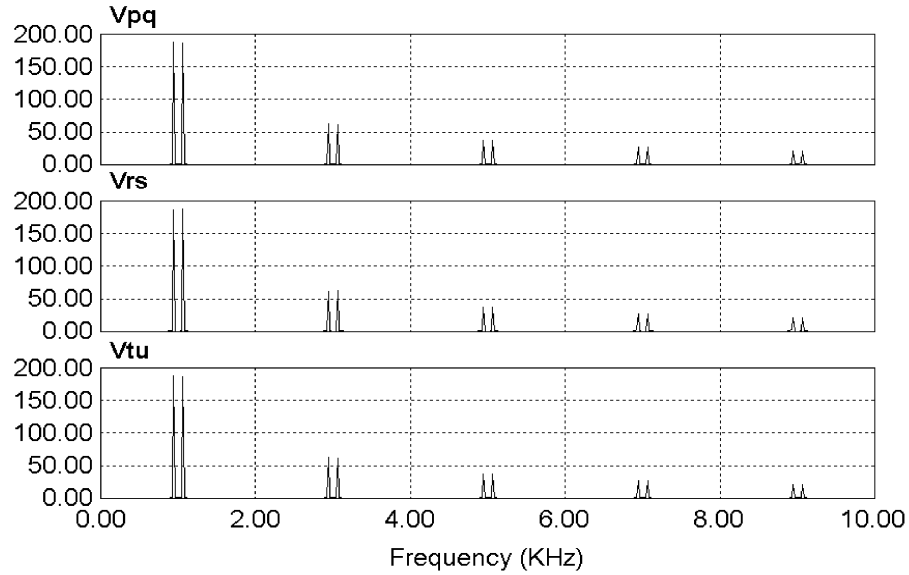

Fig. 3.8. Spectrums of high frequency voltages on transformer primary side.

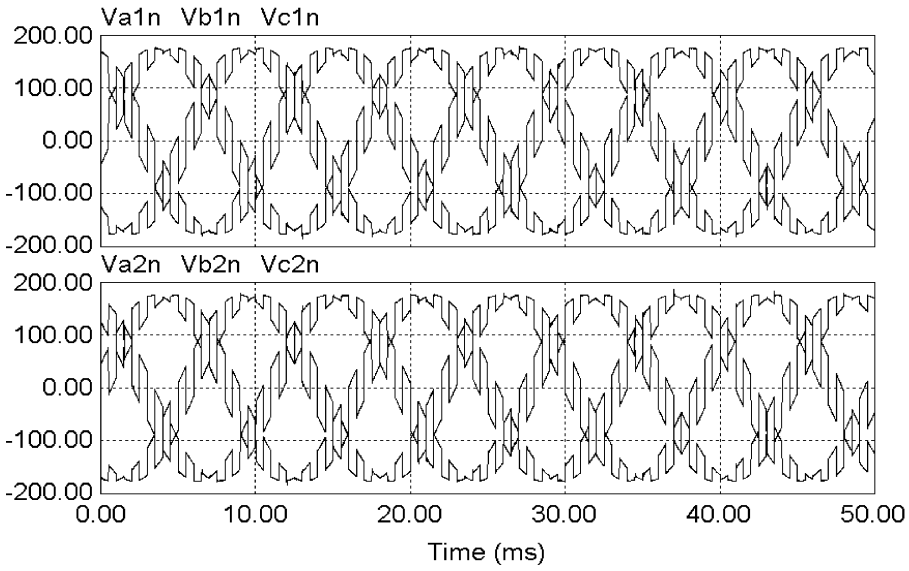

Fig. 3.9. Input voltages of the rectifier type nonlinear loads.

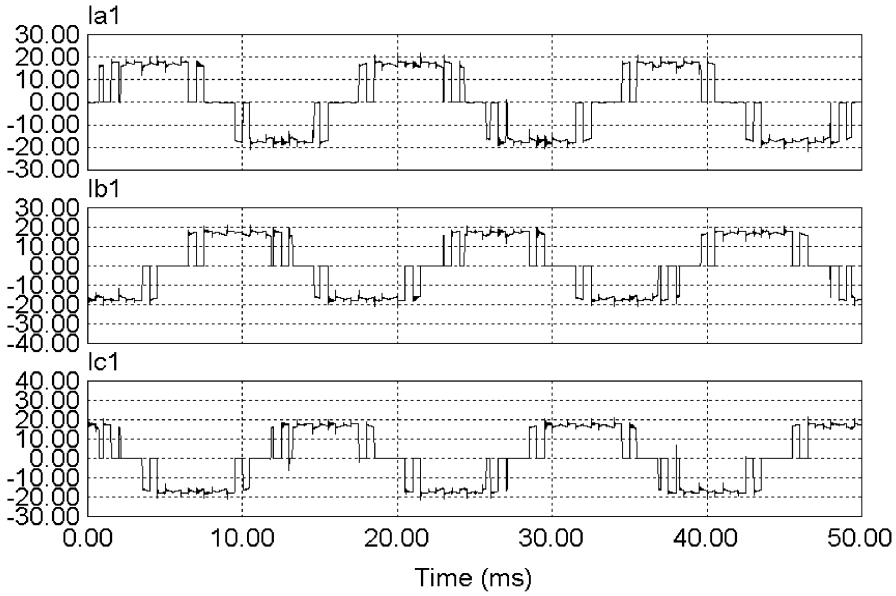

Fig. 3.10. Input currents of the rectifier type nonlinear loads.

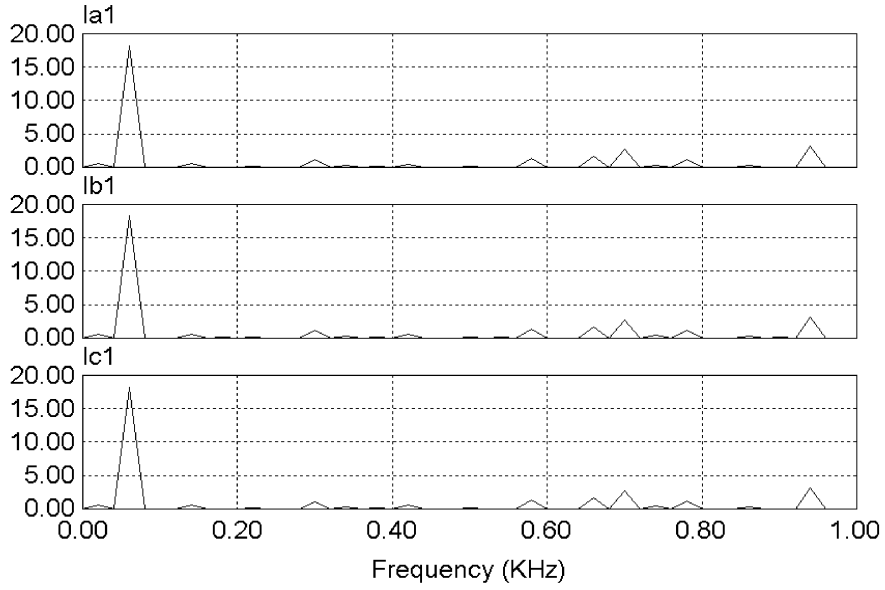

Fig. 3.11. Spectrums of input currents of the rectifier type nonlinear loads.

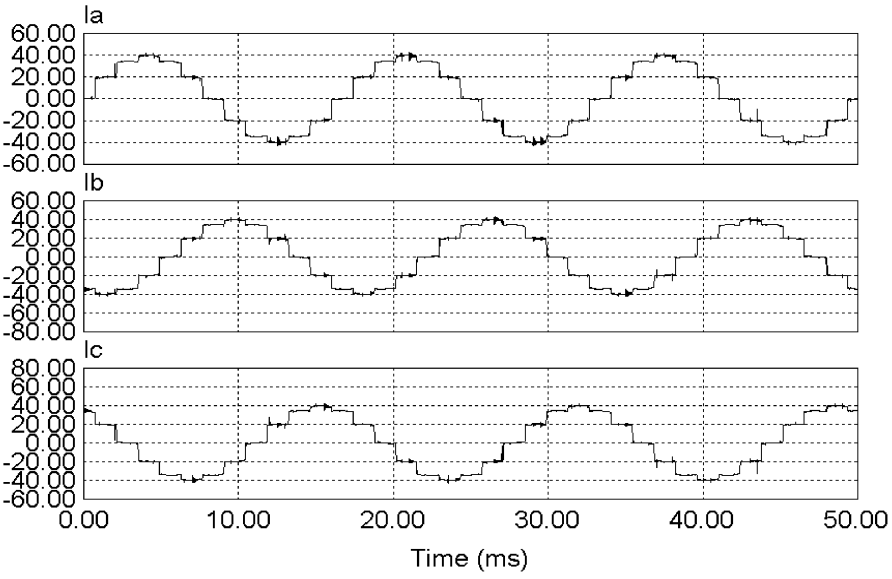

Fig. 3.12. Input line currents, I_a, I_b, and I_c of topology in Fig. 3.2.

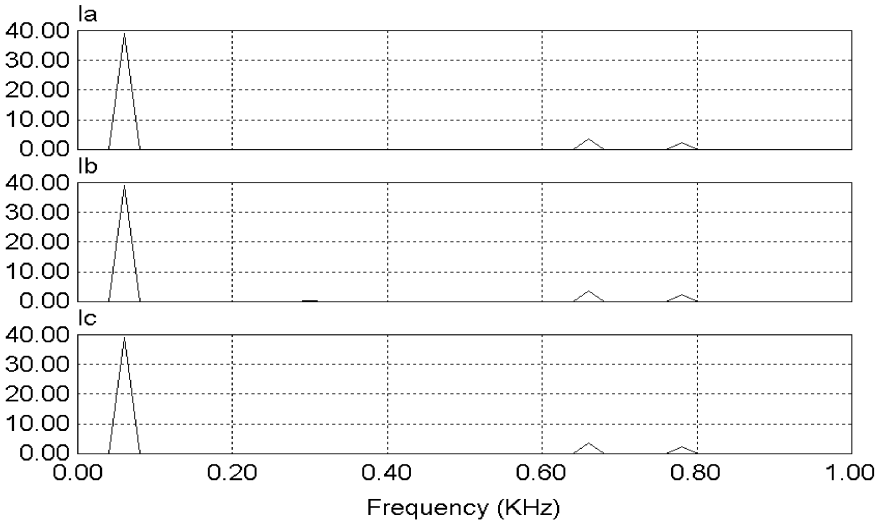

Fig. 3.13. Spectrums of input line currents (5^{th} and 7^{th} harmonics are cancelled) of topology in Fig. 3.2.

The alternative topology, as shown in Fig. 3.4, was simulated with the same input voltage of 208 V at 60 Hz, as shown in Fig. 3.6. The switching frequency of the converters was set at 1000 Hz to operate the phase-shifting transformer at high frequency. The phase-shifting voltages are achieved with the auto-connection of the transformer. Fig. 3.14 shows the sinusoidal voltages, with frequency of 60 Hz, supplied to a load with +15° phase-shifted and another one with -15° phase-shifted.

The simulation was done with rectifier type nonlinear loads. The input currents of the loads and their spectrums are shown in Fig. 3.15 and Fig. 3.16. The line input currents and their spectrums are shown in Fig. 3.17 and Fig. 3.18. The 5^{th} and 7^{th} harmonics are cancelled in the electronic transformer as they are absented. The simulation results are shown as following.

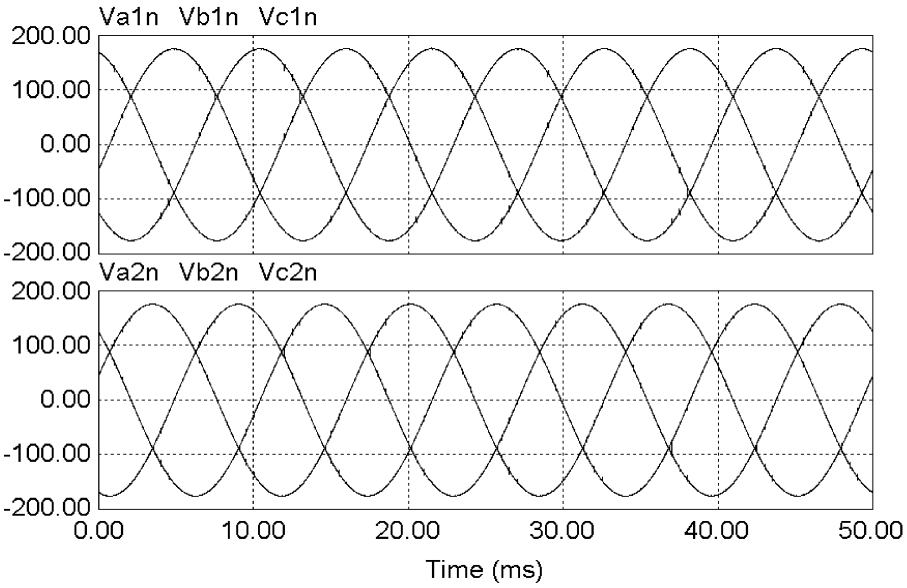

Fig. 3.14. Input voltages of the nonlinear loads without high frequency components.

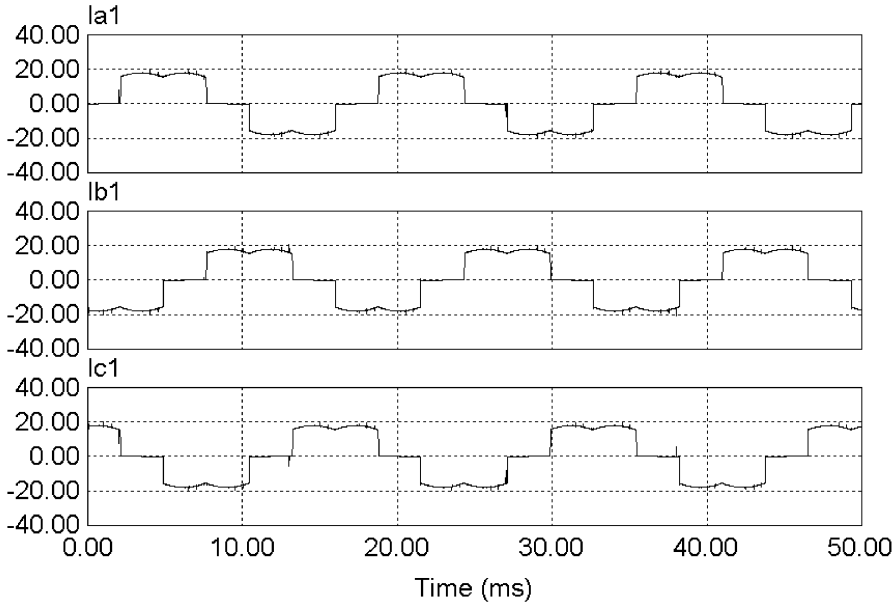

Fig. 3.15. Input currents of the nonlinear loads.

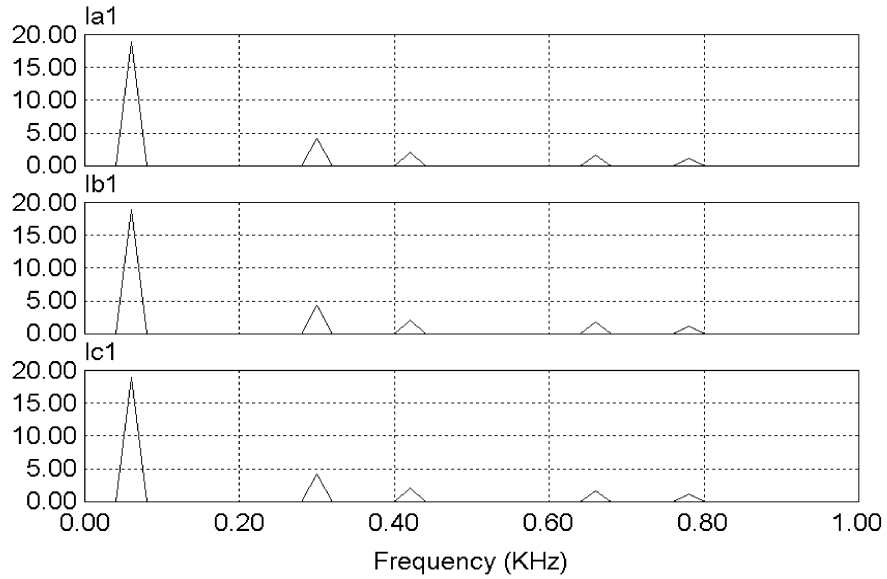

Fig. 3.16. Spectrums of input currents of nonlinear loads.

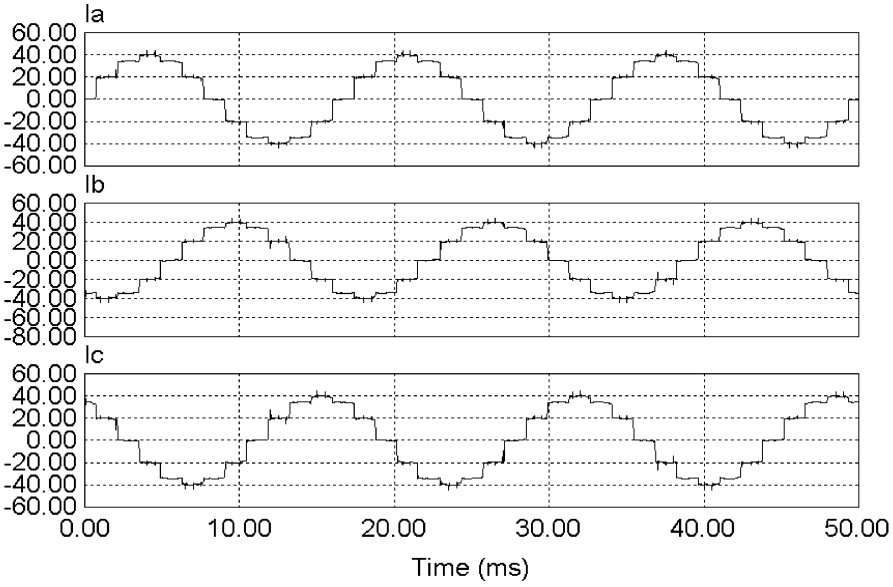

Fig. 3.17. Input line currents, I_a, I_b, and I_c of topology in Fig. 3.4.

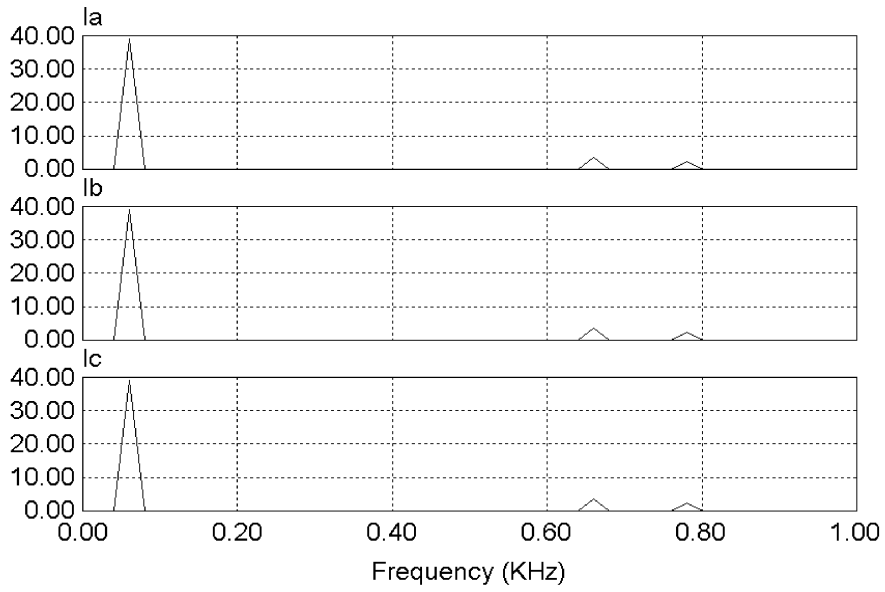

Fig. 3.18. Spectrums of input line currents (5^{th} and 7^{th} harmonics are cancelled) of topology in Fig. 3.4.

The simulation results of the proposed approach illustrate the cancellation of the 5^{th} and 7^{th} harmonics and improved current total harmonic distortion (THD), generated by nonlinear loads, in the input line currents. The simulation was done at different percentage unbalance of loads. The current THD is calculated at each stage. The graphical result, as shown in Fig. 3.19, shows that as the percentage unbalance of loads increasing, the current THD is also increasing.

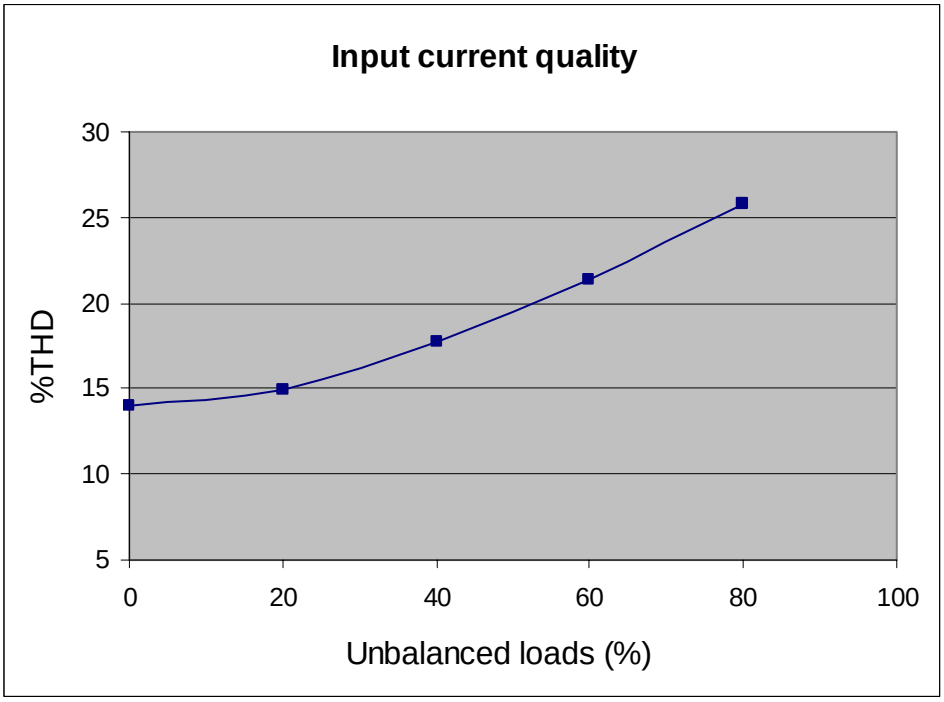

Fig. 3.19. The graphical results of THD percentage at different unbalanced loads.

3.6 Conclusion

In this chapter, the concept of employing auto-connected electronic phase-shifting transformer to cancel 5^{th} and 7^{th} harmonics in input line currents has been introduced. The results show that 5^{th} and 7^{th} harmonic currents generated by two balanced sets of nonlinear loads can be cancelled. The total harmonic distortion (THD) of utility line current has been shown in unbalanced load condition. By operating the magnetic at higher frequency, smaller size and weight can be realized.

CHAPTER IV

ELECTRONIC TRANSFORMER APPLICATION IN TELECOMMUNICATION POWER SUPPLY

4.1 Introduction

Modern telecommunication power systems require several rectifiers in parallel to obtain higher current DC output at -48 VDC [9], [20]-[22]. Commercially available telecom-rectifiers [23] employ AC to DC conversion stage with a boost converter, followed by a high frequency DC/DC converter to produce -48 VDC (see Fig. 4.1). This type of rectifier draws significant 5^{th} and 7^{th} harmonic currents resulting in near 40% total harmonic distortion (THD). In addition, the rectifier DC-link capacitor stage is bulky, contributes to weight and volume. Furthermore, the presence of multiple power conversion stages contributes to lower efficiency.

In response to these concerns, this chapter proposes a digitally controlled switch mode power supply based on a matrix converter for telecommunication applications (Fig. 4.2). Matrix converter topology employs six bi-directional switches to convert lower frequency (60/50 Hz) three-phase input directly to a high frequency (10/20 kHz) single phase output. The output is then processed via an isolation transformer and rectified to -48 VDC. Digital control of the matrix converter stage ensures that the output voltage is regulated against load changes as well as input supply variations while maintaining sinusoidal input current shape at near unity power factor.

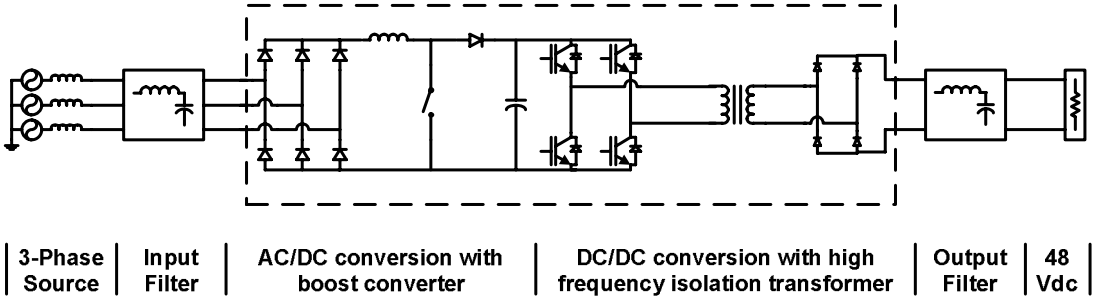

Fig. 4.1. Conventional telecommunication switch mode power supply [23].

Advantages of the proposed topology are:

- No DC-link capacitor required.
- Capable of operation over a wide input voltage range.
- Low total harmonic distortion (THD) in line current.
- Proper switching modulation results in smaller input filter.
- Unity input power factor over a wide load range.
- Higher efficiency with increased power density.
- Digital control facilitates external communication; enable parallel operation of several stages and implementation of complex closed-loop control functions.

This chapter presents a detailed analysis of the modulation scheme, discusses a design example and experimental results on a three-phase 208 V, 1.5 kW laboratory prototype converter.

4.2 Proposed switch mode power supply

The proposed digitally controlled switch mode power supply based on matrix converter is shown in Fig. 4.2. Matrix converter topology employs six bi-directional

switches to convert lower frequency (60/50 Hz) three-phase input directly to a high frequency (10/20 kHz) single phase output. The output is then processed via an isolation transformer and rectified to -48 VDC. Digital control of the matrix converter stage ensures that the output voltage is regulated against load changes as well as input supply variations.

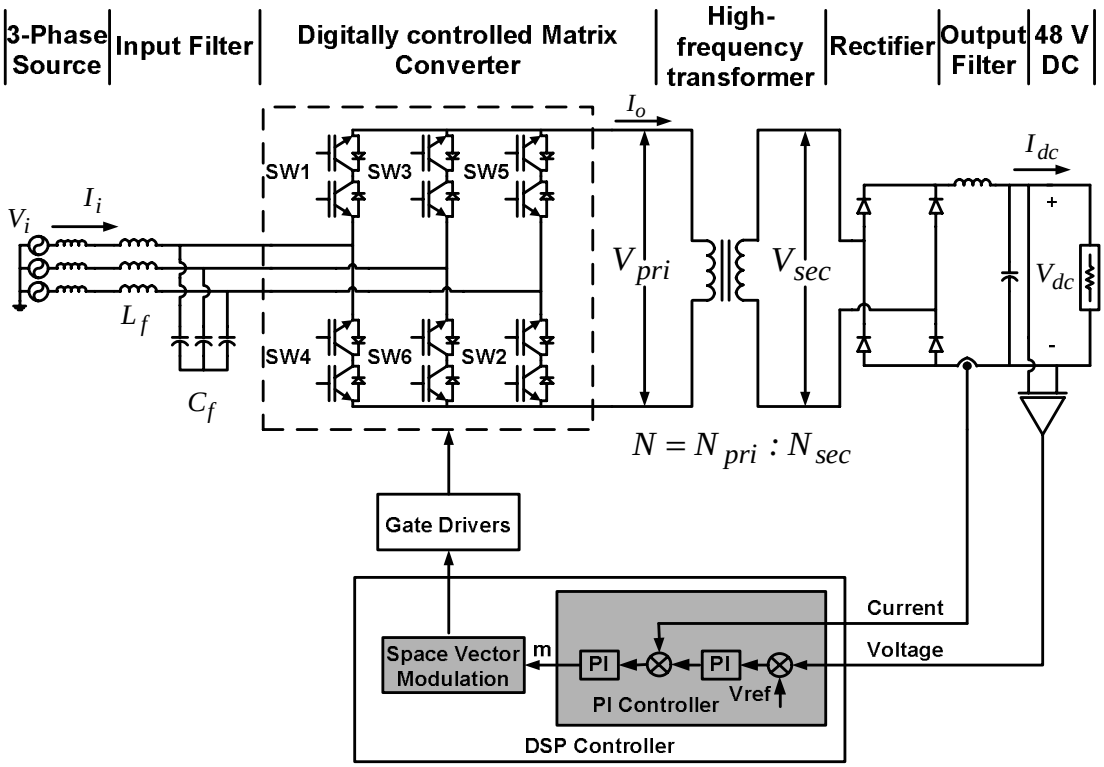

Fig. 4.2. Proposed digitally controlled switch mode power supply based on matrix converter.

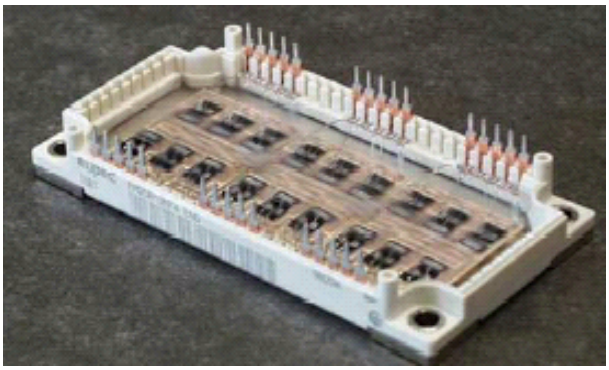

Fig. 4.3. EUPEC 18-IGBT switch module for matrix converter implementation [24].

Matrix converter is a direct AC/AC converter and operates without a DC-link [25]. It has the advantage of bidirectional power flow, controllable input power factor, high reliability, and compact design. High operating frequency of the system allows the size and weight of the transformer to be reduced. In this topology, space vector modulation technique applied to a matrix converter is employed. For hardware implementation, a three-phase to three-phase matrix converter module based on 1200V IGBT introduced by EUPEC [24] is used (see Fig. 4.3).

4.3 Matrix converter PWM modulation

In the proposed topology a three-phase to single phase matrix converter (Fig. 4.4) using twelve IGBT switches is employed.

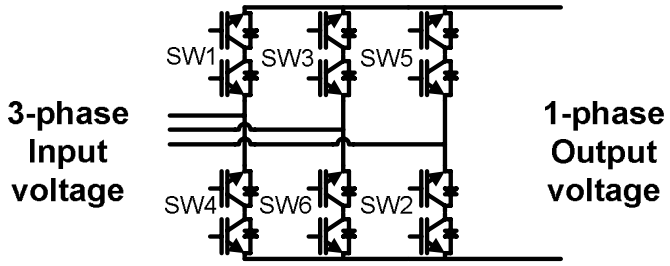

Fig. 4.4. A figure of three-phase to single phase matrix converter.

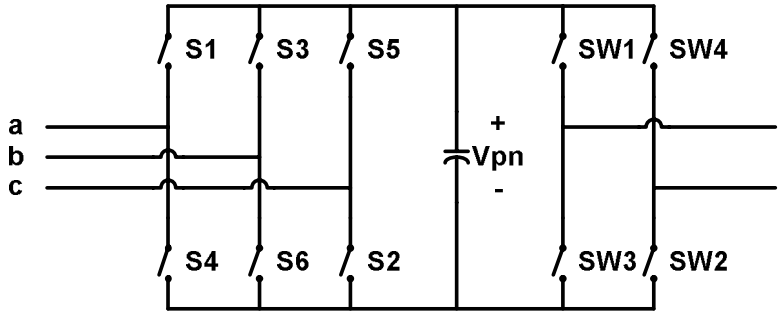

Fig. 4.5. Illustration of matrix converter operation.

The PWM modulation is divided to 2 modes, rectifier mode and inverter mode, respectively [26], [27]. Fig. 4.5 illustrates the modulation modes of matrix converter as traditional AC/DC/AC conversion system. Due to the absence of DC-link, V_{pn} is presented as a fictitious DC voltage for analysis purposes.

The operation of the matrix converter can be expressed mathematically in a matrix formation. The fictitious DC voltage, V_{pn}, is derived from the rectifier mode of operation:

$$V_{pn} = F_r * V_i \tag{4.1}$$

where F_r is rectifier mode transfer function and V_i is the input voltage vector. Matrix converter output voltage, V_o, is derived from the inverter mode of operation as follows:

$$V_o = F_i * V_{pn} \tag{4.2}$$

where F_i is the inverter mode transfer function. The line current I_i can be expressed in terms of rectifier and inverter mode transfer functions as:

$$I_i = F_r^T * F_i^T * I_o \tag{4.3}$$

The three-phase input voltage vector V_i is given by,

$$V_i = \begin{bmatrix} V_{an} \\ V_{bn} \\ V_{cn} \end{bmatrix} = \begin{bmatrix} V_m \sin(\omega_i t) \\ V_m \sin(\omega_i t - 120°) \\ V_m \sin(\omega_i t + 120°) \end{bmatrix} \tag{4.4}$$

where V_m is amplitude of input voltage and ω_i is input angular frequency.

4.3.1 Rectifier mode of operation

As detailed in the earlier section, matrix converter analysis is simplified by separating the rectifier and inverter mode of operations. The objective of the rectifier mode of operation is to create a fictitious DC voltage V_{pn} from input voltage and to maintain unity input power factor. Rectifier space vector hexagon is shown in Fig. 4.6.

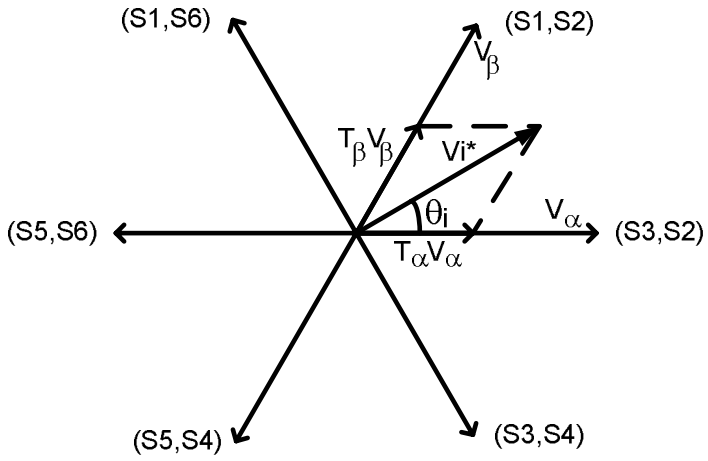

Fig. 4.6. Rectifier space vector hexagon.

The switching vectors in the hexagon in Fig. 4.6 are indicated by the switches from rectifier part in Fig. 4.5. The placement of space vector reference vector, V_i*, within one sector is defined by adjacent the switching vectors, V_α and V_β. The angle θ_i is angle of space vector reference vector. The duty cycles of the active switching vectors are calculated with rectifier mode modulation index, m_c.

$$T_\alpha = m_c \sin\left(\frac{\pi}{3} - \theta_i\right) \tag{4.5}$$

$$T_\beta = m_c \sin\left(\theta_i\right) \tag{4.6}$$

$$T_o = 1 - T_\alpha - T_\beta \tag{4.7}$$

Rectifier mode matrix, F_r, can be set up from switching functions S_1 to S_6 established by space vector method. Number of elements in F_r depends on the number of input phases.

$$F_r = [F_{r1} \quad F_{r2} \quad F_{r3}] \tag{4.8}$$

$$F_{r1} = S_1\text{-}S_4 \tag{4.9}$$

$$F_{r2} = S_3\text{-}S_6 \tag{4.10}$$

$$F_{r3} = S_5\text{-}S_2 \tag{4.11}$$

It can be stated that F_{r2} and F_{r3} are the same function as F_{r1} with phase shifting of $-\frac{2\pi}{3}$ and $+\frac{2\pi}{3}$ respectively. From (4.1) and (4.4), the fictitious DC voltage:

$$V_{pn} = 1.5 * m_c * V_m \tag{4.12}$$

4.3.2 Inverter mode of operation

The objective of this mode of operation is to generate a high frequency single phase output voltage. The operating frequency in this mode is the same as desired output frequency.

From the rectifier mode, fictitious DC voltage, V_{pn}, is found. It is used as the input of single phase inverter part in Fig. 4.5. Due to only one phase for the matrix converter output, the inverter mode matrix, F_i, has single element.

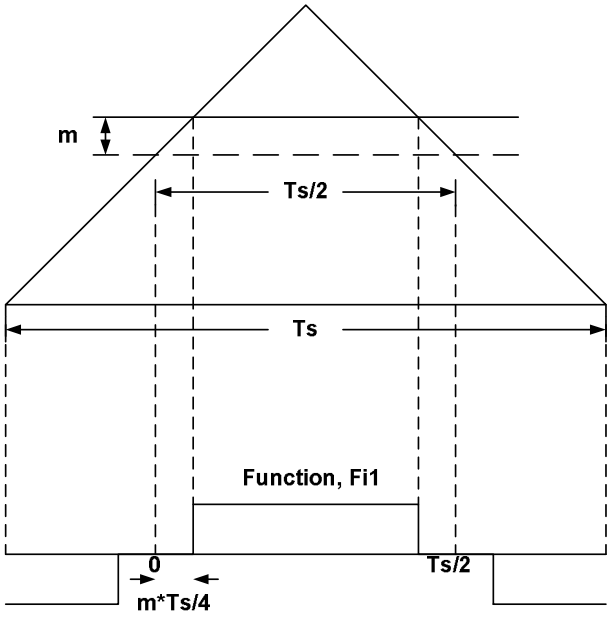

Fig. 4.7. Inverter mode switching function.

$$F_i = \left[F_{i1} \right] \tag{4.13}$$

$$F_{i1} = \text{SSW1 - SSW3 = SSW2 - SSW4} \tag{4.14}$$

The switching function, F_{i1}, can be generated as shown in Fig. 4.7. The control signal, m, is varied to obtain desired matrix converter output voltage. The switching function can be expressed as:

$$F_{i1} = \sum_{n=odd}^{\infty} B_n \sin\left(n\omega_o t\right) \tag{4.15}$$

$$B_n = \frac{4}{n*\pi} \sin\left(\frac{n\pi}{2}\right) \cos\left(n\pi\right) \sin\left(\frac{\left(m-1\right)n\pi}{2}\right) \tag{4.16}$$

From (4.2) and (4.12) and let m_v be inverter mode modulation index

$$V_o = 1.5 * m_c * m_v * V_m \tag{4.17}$$

4.3.3 Proposed switching modulation

From equation 4.1 and 4.2, it can be shown that matrix converter output can be found from:

$$V_o = F_i * F_r * V_{in} = F_T * V_{in} \tag{4.18}$$

Equation (4.18), the transfer function, F_T, is representing the matrix converter switching function. Thus, switching function of matrix converter switches can be realized as follows.

From (4.8) to (4.11), (4.13) and (4.14) we have,

$$\begin{aligned} F_T &= \begin{bmatrix} SSW_1 & SSW_3 \\ SSW_4 & SSW_2 \end{bmatrix} \times \begin{bmatrix} S_1 & S_3 & S_5 \\ S_4 & S_6 & S_2 \end{bmatrix} \\ &= \begin{bmatrix} SW_1 & SW_3 & SW_5 \\ SW_4 & SW_6 & SW_2 \end{bmatrix} \end{aligned} \tag{4.19}$$

$$\begin{aligned} SW_1 &= SSW_1 \times S_1 + SSW_3 \times S_4 \\ SW_2 &= SSW_4 \times S_5 + SSW_2 \times S_6 \\ SW_3 &= SSW_1 \times S_3 + SSW_3 \times S_6 \\ SW_4 &= SSW_4 \times S_1 + SSW_2 \times S_4 \\ SW_5 &= SSW_1 \times S_5 + SSW_3 \times S_2 \\ SW_6 &= SSW_4 \times S_3 + SSW_2 \times S_6 \end{aligned} \tag{4.20}$$

Block diagram of the proposed matrix converter modulation is shown in Fig. 4.8. Each switch can be implemented with the logic gates as shown in Fig. 4.9.

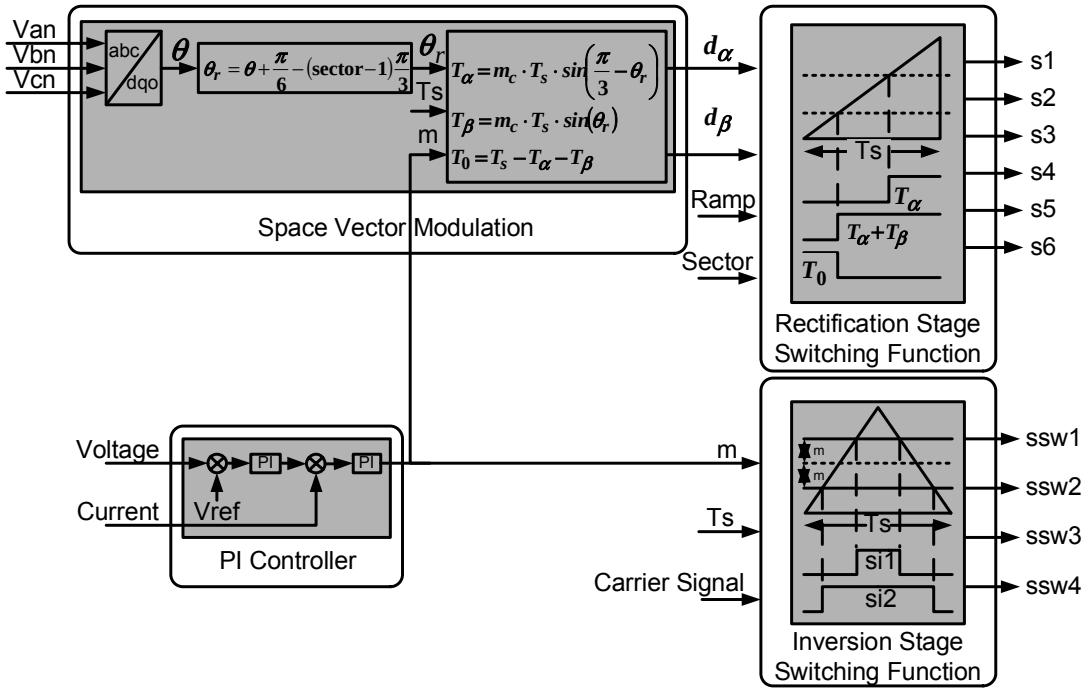

Fig. 4.8. Block diagram of the proposed matrix converter modulation.

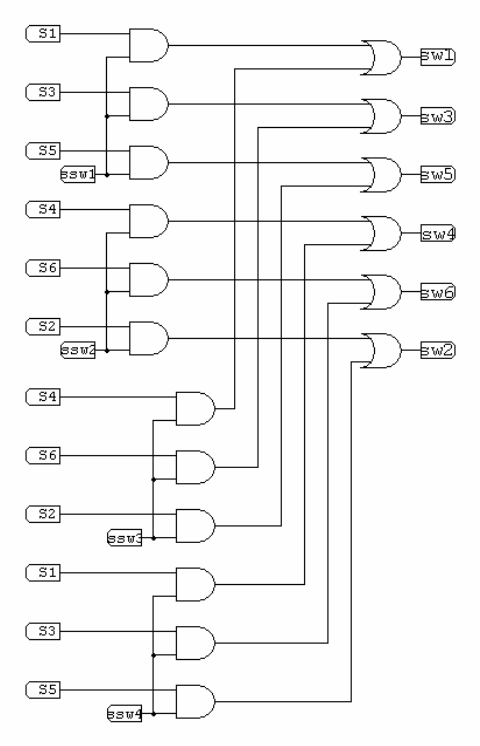

Fig. 4.9. Matrix converter switch gating signals generating through logic gates.

4.4 Analysis of the proposed power conversion stage

4.4.1 Voltage analysis

In the proposed topology, input source voltage is converted to high frequency voltage through operation of three-phase to single phase matrix converter. From (4.1) and (4.2), the matrix converter output voltage is given by,

$$V_o = F_i * F_r * V_i \tag{4.21}$$

From (4.4), (4.8) and (4.13) we have,

$$V_o(\omega_o t) = F_i * (F_{r1} * V_{ab} + F_{r2} * V_{bc} + F_{r3} * V_{ca}) \tag{4.22}$$

where

$$F_{r1} = A_1 \sin(\omega_i t) + \sum_{n=3,5,7,\ldots} A_n \sin(n\omega_i t) \tag{4.23}$$

$$F_{r2} = A_1 \sin\left(\omega_i t - \frac{2\pi}{3}\right) + \sum_{n=3,5,7,\ldots} A_n \sin\left(n\omega_i t - \frac{2\pi}{3}\right) \tag{4.24}$$

$$F_{r3} = A_1 \sin\left(\omega_i t + \frac{2\pi}{3}\right) + \sum_{n=3,5,7,\ldots} A_n \sin\left(n\omega_i t + \frac{2\pi}{3}\right) \tag{4.25}$$

Then

$$V_o(\omega_o t) = 1.5 * A_1 * B_1 * V_m \sin(\omega_o t) + V_{o,h}(\omega_o t) \tag{4.26}$$

$$\begin{aligned} V_{o,h}(\omega_o t) &= (1.5 * A_1 * V_m) \sum_{n=odd}^{\infty} B_n \sin(n\omega_o t) \\ &+ (1.5 * B_1 * V_m) \sin(\omega_o t) \sum_{n=odd}^{\infty} A_n \sin(n\omega_i t) \\ &+ (1.5 * V_m) \sum_{n=odd}^{\infty} A_n \sin(n\omega_i t) \sum_{n=odd}^{\infty} B_n \sin(n\omega_o t) \end{aligned}$$

Equation (4.26) shows no DC component in the matrix converter output voltage. The high frequency ac output voltage is connected to isolation transformer stage. In order to generate -48 VDC, the high frequency transformer performs step-down operation with suitable turn ratio, N. The selected N depends on value of input voltage and range of matrix converter modulation index and is detailed in the design example section.

4.4.2 Line current and harmonic analysis

In this section the input line current is analyzed. Equation (4.3) shows the input current I_i as a function of I_o and the rectifier/inverter mode transfer functions. Now assuming the output current I_o to be sinusoidal:

$$I_o = I_m \sin(\omega_o t) \tag{4.27}$$

where I_m is amplitude of output current and ω_o is output angular frequency.

The input current can be expressed as:

$$I_i = \begin{bmatrix} I_a \\ I_b \\ I_c \end{bmatrix} = \begin{bmatrix} F_{r1} \\ F_{r2} \\ F_{r3} \end{bmatrix} * F_{i1} * I_o \tag{4.28}$$

From (4.28), line current I_a can be expressed as,

$$I_a = F_{r1} * F_i * I_m \sin(\omega_o t) \tag{4.29}$$

Substitute (4.14) and (4.24) - (4.29) yield:

$$\begin{aligned} I_a &= \left(\frac{A_1 * B_1 * I_m}{2} \right) \sin(\omega_i t) \\ &- \left(\frac{A_1 * B_1 * I_m}{4} \right) \sin\left((\omega_i \pm 2\omega_o) t \right) + I_{a,h} \end{aligned} \tag{4.30}$$

$$\begin{aligned} I_{a,h} &= B_1 * I_m \sin^2(\omega_o t) \sum_{n=odd}^{\infty} A_n \sin(n\omega_i t) \\ &+ A_1 * I_m \sin(\omega_o t) \sin(\omega_i t) \sum_{n=odd}^{\infty} B_n \sin(n\omega_o t) \\ &+ I_m \sin(\omega_o t) \sum_{n=odd}^{\infty} A_n \sin(n\omega_i t) \sum_{n=odd}^{\infty} B_n \sin(n\omega_o t) \end{aligned}$$

where ω_i is the input frequency in rad/sec ($\omega_i = 2\pi f_i$, f_i = 60 Hz) and ω_o is the output frequency in rad/sec ($\omega_o = 2\pi f_o$, f_o = 10 kHz).

Substituting ω_i and ω_o in (4.30), it is clear that the input current does not have any low frequency harmonic components and is of high quality. The high frequency components in I_i are to be filtered by the input put filter stage of the converter.

The percentage of total harmonic distortion (THD) of utility line current is considered at input line voltage range (176 V – 264 V). Load power rating varies from 2 kW to 10 kW. The percentage of THD of the utility line currents increases as the higher input voltage is applied with trivial effect from load power. Table 4.1 shows percentage of THD of utility line currents at different input voltages where nominal input line voltage is 208 V. Fig. 4.10 shows the percentage of THD in the voltage range.

Table 4.1. %THD of input line currents at different input line voltages.

Load Power (kW)	Input line voltage (V)		
	176	208	264
10	2.829 %	3.090 %	3.532 %

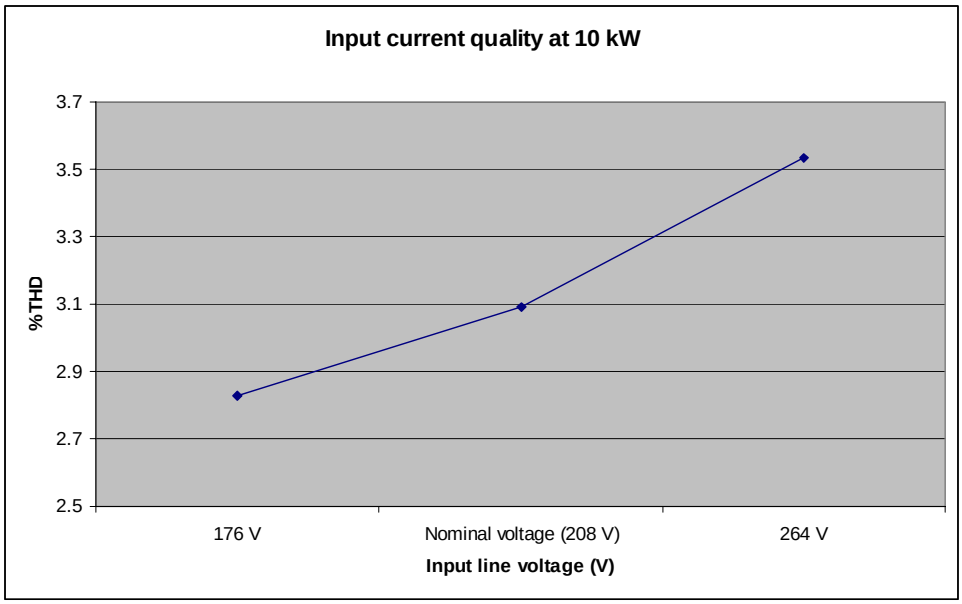

Fig. 4.10. %THD of input line currents at different input line voltages.

4.5 Design example

In this section a design example is presented. To facilitate calculation in per-unit, the following base quantities are defined.

$$P_{base} = P_o = 1.5 \text{ kW}$$

$$V_{base} = V_{dc} = 48 \text{ V}$$

$$I_{base} = I_{dc} = 31.25 \text{ A}$$

$$Z_{base} = \frac{V_{base}}{I_{base}} = 1.536\ \Omega$$

Input line voltage V_i = 4.33 per-unit.

The matrix converter output current I_o is given by,

$$I_o = \frac{1}{N} * I_{dc} \tag{4.31}$$

where N is the transformer turn ratio.

Select N = 4, I_o = 0.25 per-unit.

Neglecting losses, the utility line current can be expressed as:

$$I_a = \frac{P_o}{\sqrt{3} * V_i} \tag{4.32}$$

And the input current I_a = 0.133 per-unit.

The input and output specifications of the design are shown in Table 4.2.

Table 4.2. Design specifications of the proposed approach.

Design specifications	Values
Input line voltage (V_i)	208 V
Input frequency (f_i)	60 Hz
Switching frequency (f_{sw})	10 kHz
Output DC voltage (V_{dc})	48 V
Load power (P_o)	1.5 kW
Matrix converter module 1200V	12 IGBTs

4.5.1 Input filter design

High frequency current components in the input current of matrix converter can be filtered via a LC filter. The value of filter capacitor is selected by the following equation [28].

$$C_F \approx \frac{2*P}{3*V_m{}^2*\omega_i} \tag{4.33}$$

where P is the power rating, V_m is the peak of input voltage, and ω_i is angular input frequency.

The value of filter inductor is chosen by,

$$L_F = \frac{1}{(2\pi f_o)^2 * C_F} \tag{4.34}$$

where f_c is the cut-off frequency and is chosen to be lower than the switching frequency (10 kHz). With the parameter values given in this design example, and cut-off frequency is chosen to be 1.7 kHz:

Filter capacitance (C_F) = 60 μF.

Filter inductor (L_F) = 150 μH.

4.6 Simulation results

In this section simulation results of the proposed approach are discussed. Fig. 4.11 shows the three-phase input line voltages. Fig. 4.12 shows the high frequency output voltage of the matrix converter. Fig. 4.13 shows the 48 V DC output voltage. Fig. 4.14 illustrates the performance of the proposed converter from utility perspective. It is clear for these results that input current is of high quality and is in phase with the input line to neutral voltage. Fig. 4.15 shows the variation of input current THD as a function of load.

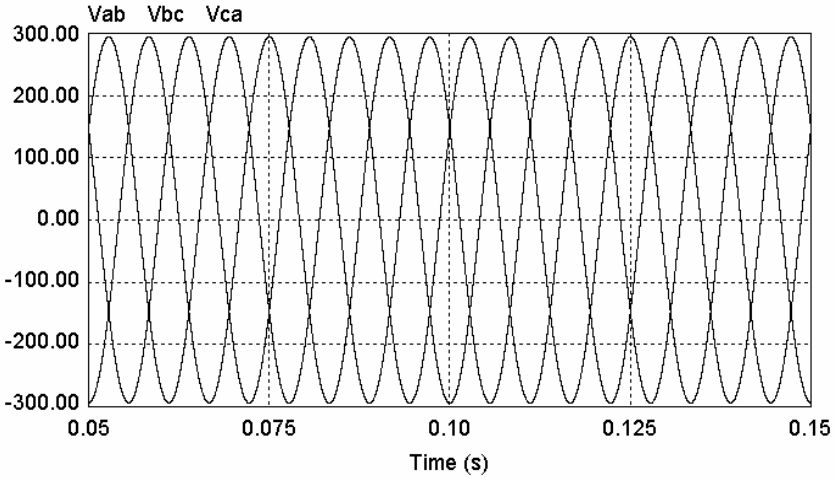

Fig. 4.11. The three-phase input voltages V_{ab}, V_{bc}, and V_{ca} : 208 V (rms) 60 Hz.

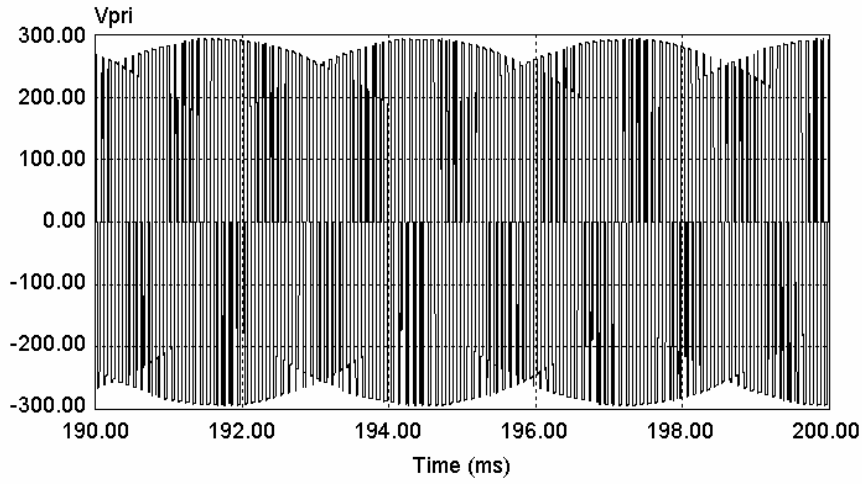

Fig. 4.12. High frequency output voltage V_{pri} of the matrix converter.

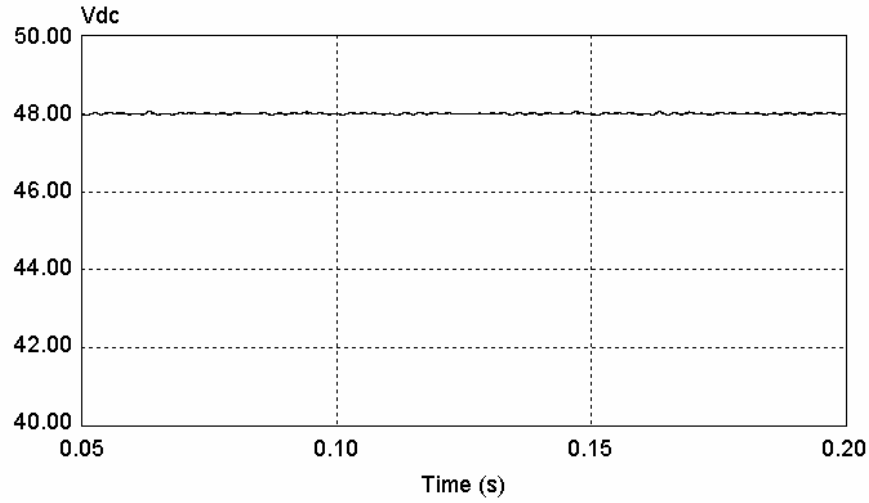

Fig. 4.13. Output DC voltage (48 V).

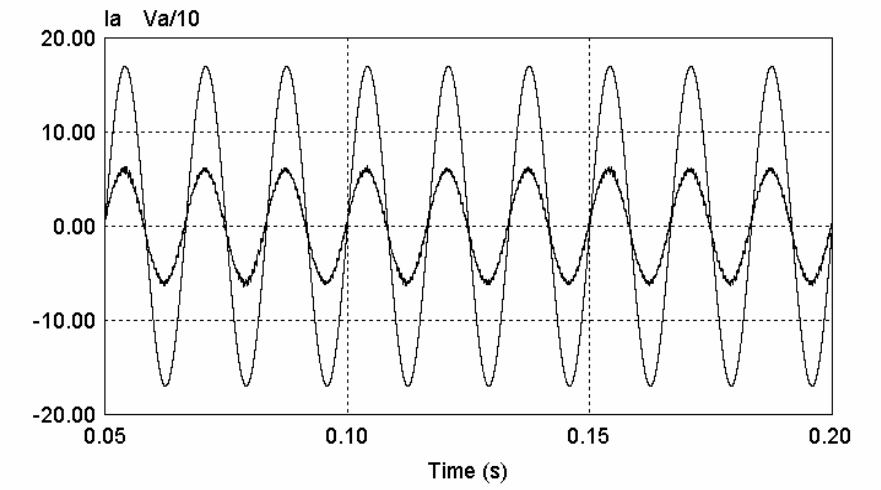

Fig. 4.14. Input line to neutral input voltage V_{an} and input current I_a.

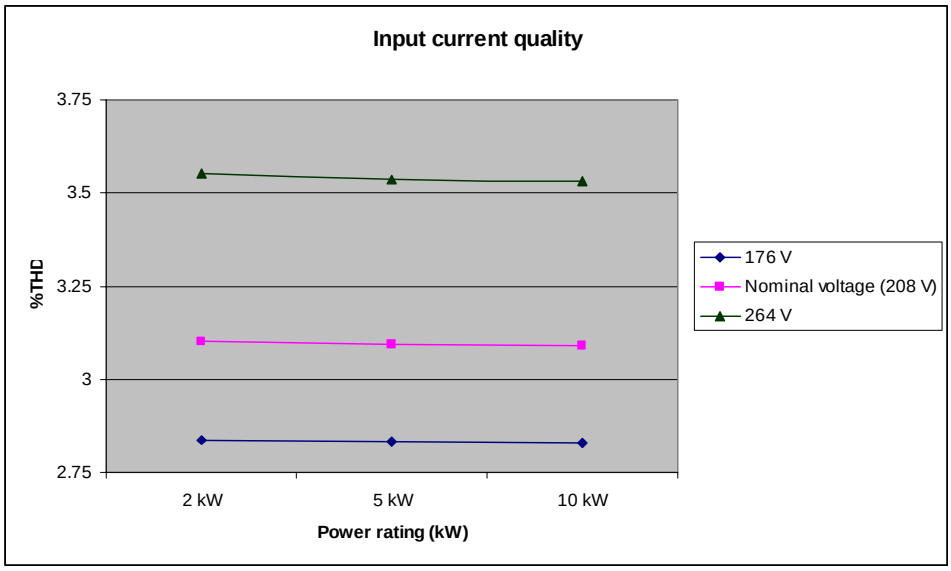

Fig. 4.15. THD percentage at different loads.

4.7 Experimental results

A laboratory prototype of the proposed digitally controlled switch mode power supply was constructed to meet the specifications detailed in section 4.5. A commercially available matrix converter module: FM35R12KE3 from EUPEC [22] was employed. A digital signal processor (TMS320LF2407) was used for generating PWM gating signals and performing closed loop functions. Fig. 4.16 shows the prototype matrix converter unit. The unit is connected to bridge rectifier, which consists of 4 fast-recovery diodes (60EPU02), and an output filter to produce power supply voltage of 48 V DC. Fig. 4.17 shows the input voltage V_{ab}, matrix converter output voltage (high frequency) V_{pri} (connected to the transformer primary winding) and the transformer secondary voltage V_{sec}. Fig. 4.18 shows the transformer primary and secondary voltages with expanded time scale. Fig. 4.19 shows the output DC voltage (48 V) and the load current. Fig. 4.20 shows the line to neutral voltage V_{an} and the line current I_a at 1.5 kW output power. It is clear that the input current is of high quality and unity power factor.

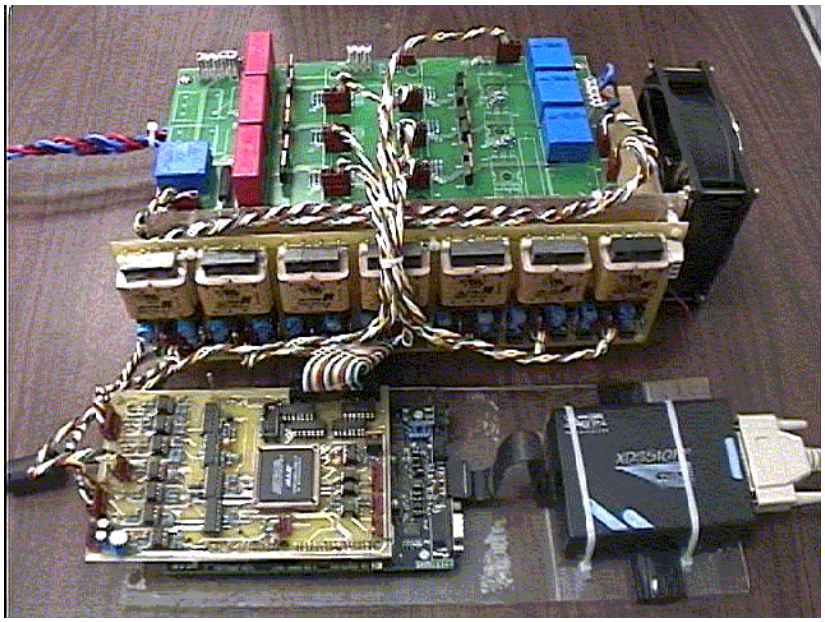

Fig. 4.16. Proposed matrix converter prototype.

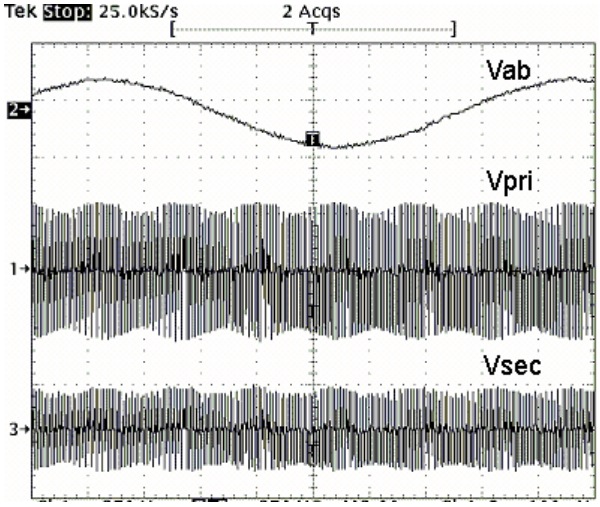

Fig. 4.17. Input voltage V_{ab}, matrix converter output voltage V_{pri}, and transformer secondary voltage V_{sec}.

(1: V_{pri} [500 V/div], 2: V_{ab} [250 V/div], 3: V_{sec} [50 V/div])

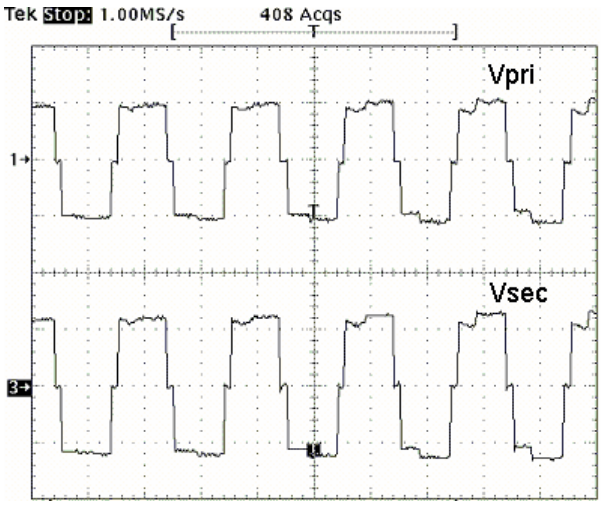

Fig. 4.18. Transformer primary V_{pri} and secondary voltages V_{sec}.

(1: V_{pri} [250 V/div], 3: V_{sec} [25 V/div])

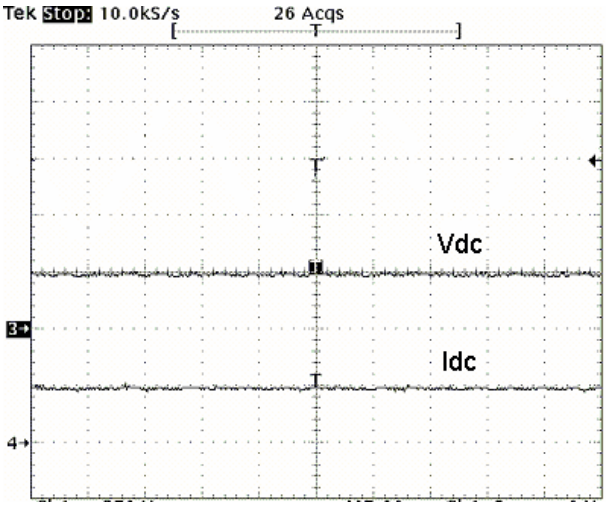

Fig. 4.19. Output DC voltage V_{dc} and load current I_{dc}.

(3: V_{dc} [50 V/div], 4: I_{dc} [10 A/div])

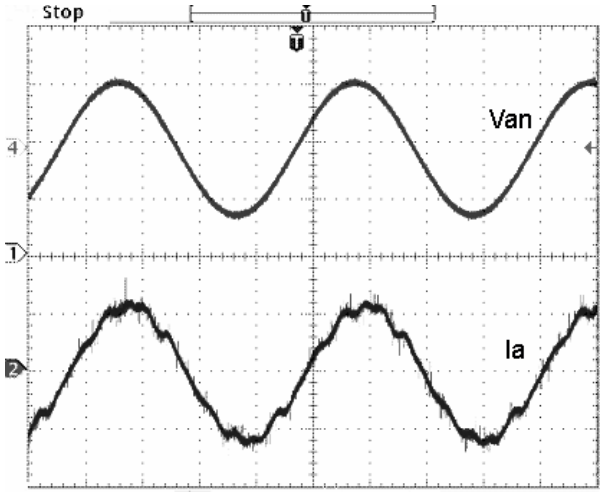

Fig. 4.20. Input line to neutral voltage V_{an} and the input line current I_a at 1.5 kW of output power.

(1: V_{an} [100 V/div], 2: I_a [5 A/div])

4.8 Conclusion

In this chapter a digitally controlled switch mode power supply based on matrix converter for telecommunication applications has been shown. The proposed space vector PWM method has been shown to yield high quality input current for varying load conditions. Experimental results on a 1.5 kW prototype have demonstrated the feasibility of a direct AC to AC matrix converter in telecommunication power supplies.

CHAPTER V

CONCLUSION

In this dissertation, applications of electronic transformer in power distribution system have been presented. The concept of electronic transformer operating at higher frequency has been shown to effectively achieve size, weight, and volume reduction of transformer. The single phase and three-phase electronic transformer systems have been explained and analyzed.

The extended study on a concept of auto-connected electronic phase-shifting transformer has been presented to reduce total harmonic distortion (THD) in utility line currents generated by nonlinear loads. Two configurations of the auto-connected electronic phase-shifting transformer have been shown and analyzed. In both configurations, high frequency operation was achieved through power electronic converter on transformer primary side. In the first configuration, power electronic converter was absent from transformer secondary side. The analysis has shown that 5^{th} and 7^{th} harmonics generated by 2 nonlinear loads were cancelled despite of the balance of loads. However, at unbalanced load condition, total harmonic distortion (THD) of utility line current has been shown to be higher than the balanced load condition due to sub-harmonics generated by switching frequency. The 10 kVA auto-connected electronic phase-shifting transformer system was operated at 1 kHz. At balanced load condition, the system showed the THD of utility line current at 13.79%, while at 40% unbalanced load condition the THD was 17.35%.

The second configuration of auto-connected electronic phase-shifting transformer consists of secondary converters. The analysis has shown that, at balance load condition, 5^{th} and 7^{th} harmonics generated by 2 nonlinear loads were cancelled. Alternatively, at unbalanced load condition, 5^{th} and 7^{th} harmonics were not cancelled and caused incretion in the total harmonic distortion (THD) of utility line current. The second configuration showed the THD of utility line current of 13.97% at balanced load condition. At 40% unbalanced load condition, the THD was 17.71%. Simulation results of both configurations are shown.

Finally, a digitally controlled matrix converter based switch mode power supply for telecommunication application has been presented. The proposed space vector PWM method on matrix converter has been shown to yield high quality input current for varying load conditions. The power supply was designed to be operated in the range of input utility line voltage of 176 V to 264 V. The varying of loads, at the same input voltage, did not show effect on the quality of input current as the total harmonic distortion (THD) was not changed. However, operating the power supply at higher input voltage caused higher total harmonic distortion (THD) in utility line current. Simulation results have been presented along with design example. Experimental results on a 1.5 kW prototype have demonstrated the feasibility of a direct AC/AC matrix converter in telecommunication power supplies.

For future work, solid state power substation (SSPS) concept can be further developed with electronic transformer. Voltage transformation, voltage regulation, non-standard customer voltages (DC or 400 Hz AC), voltage sag correction, power

factor control, and distribution system status monitoring to facilitate automation can be achieved through digital control of direct AC to AC converter. Due to the indication of higher heat dissipation in high frequency transformer, further study on transformer size reduction should focus on possibility of reducing the loss as well. Addressing packaging and cooling system related to electronic transformer could be pursued. Application of high temperature devices such as silicon carbide MOSFETs and diodes could further the electronic transformer and SSPS concepts.

REFERENCES

[1] M. Kang, P. N. Enjeti, and I. J. Pitel, "Analysis and design of electronic transformers for electric power distribution system," *IEEE Trans. Power Electronics*, vol.14, no. 6, pp. 1131-1141, Nov. 1999.

[2] S. D. Sudhoff, "Solid state transformer," U.S. Patent 5,943,229, August 24, 1999.

[3] T. Wildi, *Electrical Machines, Drives, and Power Systems*. Upper Saddle River, NJ: Prentice Hall, 1999.

[4] E. V. Larsen, "A classical approach to constructing a power flow controller," presented at IEEE Power Engineering Society Summer Meeting, Alberta, Canada, Jul. 1999.

[5] B. Sweeney, "Application of phase-shifting transformers for the enhanced interconnection between Northern Ireland and the Republic of Ireland," *Power Engineering Journal*, pp. 161-167, Jun. 2002.

[6] D. A. Paice, *Power Electronic Converter Harmonics - Multipulse Methods for Clean Power*. New York: IEEE Press, 1996.

[7] S. Choi, P. Enjeti, and I. Pitel, "Polyphase transformer arrangements with reduced KVA capabilities for harmonic current reduction in rectifier type utility interface," *IEEE Trans. Power Electronics*, vol. 11, no. 5, pp. 680-690, Sept. 1996.

[8] M. Kang, B. O. Woo, P. Enjeti, and I. Pitel, “Auto-connected electronic transformer (ACET) based multi-pulse rectifiers for utility interface of power electronic systems,” *IEEE Trans. Ind. Applicat.*, pp. 646-656, May/June, 1999.

[9] P. Enjeti, and S. Kim, “A new dc-side active filter for inverter power supplies compensates for unbalanced and nonlinear load,” in *Proc. IEEE IAS Conf.*, Oct. 1991, pp. 1023-1031.

[10] Electric Power Research Institute, “Intelligent universal transformer technology development,” Apr. 2004, available at http://www.epri.com.

[11] N. Mohan, T. M. Undeland, and W. P. Robbins, *Power Electronics Converters, Applications, and Design.* New York: John Wiley & Sons, Inc., 1995.

[12] P. N. Enjeti, and S. Choi, “An approach to realize higher power ac controller,” in *Proc. IEEE APEC Conf.*, Mar. 1993, pp. 323-327.

[13] E. R. Ronan, S. D. Sudhoff, S. F. Glover, and D.L. Galloway, “A power electronic-based distribution transformer,” *IEEE Trans. Power Delivery*, vol. 17, no. 2, pp. 537-543, Apr. 2002.

[14] E. C. Aeloiza, P. N. Enjeti, L.A. Morán, and I. Pitel, “Next generation distribution transformer: to address power quality for critical loads,” in *Proc. IEEE PESC Conf.*, vol. 3, Jun. 2003, pp. 1266-1271.

[15] J. Kammeter, “Harmonic cancellation system,” U.S. Patent 5,434,455, July 18, 1995.

[16] T. Gruzs, “Harmonics current reduction techniques for computer systems,” Liebert Corp., Sept. 2003, available at http://www.liebert.com.

[17] J. Kammeter, “Transformer with cancellation of harmonics currents by phase shifted secondary windings,” U.S. Patent 5,206,539, April 27, 1993.

[18] M. Levin, “Phase shifting transformer with low zero phase sequence impedance,” U.S. Patent 5,982,262, November 9, 1999.

[19] M. Kang, P. Enjeti, and I. Pitel, “A simplified auto-connected electronic transformer (SACET) approach upgrades standard 6-pulse rectifier equipment with 12-pulse characteristics to facilitate harmonic compliance,” in *Proc. IEEE PESC Conf.*, vol. 1, 1999, pp. 199-204.

[20] A. I. Pressman, *Switching Power Supply Design*. New York: McGraw-Hill, 1997.

[21] A. W. Lotfi, “Issues and advances in high-frequency magnetics for switching power supplies,” *IEEE Proceedings*, vol. 89, no. 6, pp. 833-845, June 2001.

[22] R. Redl, and A. S. Kislovski, “Telecom power supplies and power quality,” in *Proc. INTELEC Conf.*, Nov. 1995, pp. 13-21.

[23] Tyco Electronics, “Galaxy Switchingmode Rectifier 595 Series,” Datasheet, Feb. 2003, available at http://www.tycoelectronics.com.

[24] M. Hornkamp, M. Loddenkötter, M. Münzer, O. Simon, and M. Bruckmann, “EconoMAC the first all-in-one IGBT module for matrix converters,” EUPEC, available at http://www.eupec.com [Accessed May 2004].

[25] M. Venturini, “A new sine wave in, sine wave out, conversion technique eliminates reactive element,” in *Proc. POWERCON 7*, Mar. 1980, pp. E3_1-E3_15.

[26] L. Huber, and D. Borojevic, “Space vector modulated three-phase to three-phase matrix converter with input power factor correction,” *IEEE Trans. Ind. Applicat.*, vol. 31, no. 6, pp. 1234-1246, Nov./Dec.1995.

[27] H. J. Cha, and P. N. Enjeti, “A three-phase AC/AC high-frequency link matrix converter for VSCF applications,” in *Proc. IEEE PESC Conf.*, vol. 4, Jun. 2003, pp. 1971-1976.

[28] C. L. Neft and C. D. Schauder, “Theory and design of 30-hp matrix converter”, *IEEE Trans. Ind. Applicat.*, vol. 28, no. 3, pp. 546-551, May/June 1992.

APPENDIX

Current distortion is defined by the total harmonic distortion (THD), which is the relationship between total harmonic currents I_n and the fundamental current I_L as shown in (A.1).

$$THD = \frac{\sqrt{\sum_{n=2}^{40} (I_n)^2}}{I_L} \tag{A.1}$$

IEEE standard 519-1992 recommends harmonic current limits for 120 V – 69 kV systems as shown in Table A.1.

Table A.1. IEEE standard 519-1992 for 120 V - 69 kV systems.

Maximum Harmonic Current Distortion in Percent of I_L						
Individual Harmonic Order (Odd Harmonics)						
I_{sc} / I_L	h < 11	11 ≤ h < 17	17 ≤ h < 23	23 ≤ h < 35	35 ≤ h	THD
< 20	4.0	2.0	1.5	0.6	0.3	5.0
20 < 50	7.0	3.5	2.5	1.0	0.5	8.0
50 < 100	10.0	4.5	4.0	1.5	0.7	12.0
100 < 1000	12.0	5.5	5.0	2.0	1.0	15.0
> 1000	15.0	7.0	6.0	2.5	1.4	20.0
Even harmonics are limited to 25% of the odd harmonic limits above.						
Current distortion that result in a dc offset, e.g., half-wave converters, are not allowed.						
*All power generation equipment is limited to these values of current distortion., regardless of actual I_{sc} / I_L						
where I_{sc} = maximum short-circuit current at PCC. I_L = maximum demand load current (fundamental frequency component) at PCC.						

VITA

Somnida Ratanapanachote was born in Bangkok, Thailand in 1974. She received her B.Eng. degree in electrical engineering from Mahidol University in May 1995. Later, she received a scholarship for graduate studies from the Thai government. She attended Texas A&M University in 1996 and received her M.Eng. degree in electrical engineering in May 1998. She started her doctoral program in electrical engineering at Texas A&M University in 1998 and received her Ph.D. in electrical engineering in August 2004. Her area of interest is in power electronics and power quality. She can be reached at: 53/55 Lad Phrao 15, Jatujak, Bangkok 10900 Thailand or somnida@hotmail.com.